Heliyon 10 (2024) e28260

Contents lists available at ScienceDirect

Heliyon

journal homepage: www.cell.com/heliyon

Research article

A QSPR analysis of physical properties of antituberculosis drugs using neighbourhood degree-based topological indices and support vector regression

Muhammad Shafii Abubakar [a], Kazeem Olalekan Aremu [a,b,*], Maggie Aphane [a], Lateef Babatunde Amusa [c]

[a] Department of Mathematics and Applied Mathematics, Sefako Makgatho Health Sciences University, P.O. Box 60, 0204, Pretoria, South Africa
[b] Department of Mathematics, Usmanu Danfodiyo University Sokoto, P.M.B. 2346, Sokoto State, Nigeria
[c] Department of Statistics, University of Ilorin, P.M.B. 1515, Ilorin, Kwara State, Nigeria

ARTICLE INFO

MSC:
05C07
05C90
05C92

Keywords:
Neighbourhood degree-based topological indices
QSPR analysis
Antituberculosis drugs
Support vector regression

ABSTRACT

Topological indices are molecular descriptors used in QSPR modelling to predict the physico-chemical properties of molecules. Topological indices are used in numerous applications in drug design. In this work, we compute the neighbourhood degree-based topological indices of 15 anti-tuberculosis drugs, we studied the QSPR analysis of these drugs using support vector regression. The efficiency of support vector regression is determined by comparing it with the classical linear regression. Our QSPR model further shows the superiority of the SVR model as a better predictive model in QSPR analysis of the physical properties of antituberculosis drugs. The findings in this study are a further contribution to the field of chemical graph theory and drug design, providing a deeper understanding of neighbourhood degree-based topological indices and their predictive capabilities in QSPR model.

1. Introduction

Tuberculosis, often referred to as TB, is a communicable disease caused by bacillus Mycobacterium tuberculosis (Mtb). It was the world's infectious disease with the most death rate until the Coronavirus (COVID-19) pandemic in 2020. TB primarily affects the lungs of the infected patient, it also affects other organs of the body such as the kidneys and lymph nodes. TB is commonly transmitted through the air mostly when infected people cough or sneeze thereby expelling the bacteria into the atmosphere. It has been estimated by the World Health Organization (WHO) global TB report [49] that about a quarter of the global population is estimated to have been infected with TB and 90% of the majority of those infected are adults, without quick treatment, 50% of the infected population end up losing their lives but with the current recommended treatment which involves 4-6 months of antituberculosis drugs dosage, 85% of the infected population can be cured. TB has been responsible for the death of over 1.4 million infected people worldwide which includes deaths attributed to higher immune virus-tuberculosis (HIV-TB) co-infection, this is due to similarities in symptoms between HIV and TB. According to the First National TB Prevalence Survey [47] conducted in South

* Corresponding author at: Department of Mathematics, Usmanu Danfodiyo University Sokoto, P.M.B 2346, Sokoto, Nigeria.
E-mail address: aremukazeemolalekan@gmail.com (K.O. Aremu).

https://doi.org/10.1016/j.heliyon.2024.e28260
Received 25 October 2023; Received in revised form 5 March 2024; Accepted 14 March 2024

Available online 20 March 2024
2405-8440/© 2024 Sefako Makgatho Health Sciences University. Published by Elsevier Ltd. This is an open access article under the CC BY-NC-ND license (http://creativecommons.org/licenses/by-nc-nd/4.0/).

Africa in 2018, South Africa is one of the 30 high burden TB countries in the world contributing 87% of the estimated incident of TB cases worldwide. TB can be diagnosed via a series of methods, Konstantinos [25] discusses diagnostic tests for TB such as analyzing sputum specimens for mycobacteria to diagnose active TB, tuberculin skin testing for diagnosing latent TB and the use of interferon gamma release assays in certain cases. Factors associated with death were examined by Ulugbek [37] in hospitalized pulmonary tuberculosis patients with acute respiratory failure. The study discovered that the following conditions were predictive of death: advanced age, positive acid-fast bacilli smear, severe chest radiograph, pneumonia, diabetes, low albumin, sepsis, and multiorgan failure, concluding that knowledge of these variables can enhance pulmonary tuberculosis patient's care and management. Flynn and Chan [19] further explored the complex immune response to Mtb infection and highlight the heterogeneity of the outcomes. The study emphasized on the need for a holistic approach that considers the interactions between Mtb and various host cells. They further discussed the role of granulomas in the immune response and stress the importance of understanding the collective immune responses rather than focusing on individual components. (See [13,22,27] for more details on TB in general.)

In recent years, there has been an urgent need to develop a novel mycobacterium chemotherapeutics to overcome the challenges posed by TB due to multi-drug resistant that the mycobacterium develops over time when a patient is on treatment [4]. This has led researchers to develop novel laboratory and theoretical approaches to combat the threat that TB posses to the human and animal population in today's world. So far, progress is being made, the most obvious impact of the fight against TB was a large global drop in the reported number of newly diagnosed people with TB, from a peak of 7.1 million infections in 2019 to 5.8 million in 2020, although this numbers rose up to 6.4 million in 2021, this was due to the COVID-19 damaging impact on access to TB diagnoses and treatment (see WHO report 2022 [48]). Globally, the estimated number of deaths from TB increased between 2019 and 2021. The progress made so far is attributed to the development of laboratory antituberculosis drugs such as amikacin, bedaquiline, ethambutol, ethionamide, isoniazid, moxifloxacin etc. Feng et al. [18] examined the adoption of shorter regimens for treating latent tuberculosis infection in the United States. The analysis reveals a trend towards the use of abbreviated treatment regimens, such as 4 months of rifampin or 12 weeks of isoniazid and rifapentine. The study emphasizes the improved tolerability and completion rates of these regimens compared to the previously recommended longer courses of treatment. Van Schalkwyk [38] investigated the impact of pregnancy on the pharmacokinetics of first-line tuberculosis drugs. Rifampin and pyrazinamide concentrations were comparable during pregnancy and postpartum, while isoniazid and ethambutol concentrations were lower during pregnancy. The median area under the curve values for rifampin, isoniazid, and pyrazinamide met therapeutic targets. Their findings emphasize the importance of understanding drug exposure during pregnancy and highlight the need for further research to determine the clinical implications and optimize dosing guidelines for pregnant individuals with tuberculosis. Anzueto et al. [5] compared moxifloxacin and levofloxacin for treating other repiratory disease such as pneumonia in elderly patients. Moxifloxacin was found to be effective and safe, with higher cure rates and faster clinical recovery than levofloxacin. Both drugs had comparable safety profiles. The findings support moxifloxacin as a treatment option for elderly patients with pneumonia.

The process of designing drugs in a laboratory is time-consuming and expensive. However, this lengthy process can be reduced by employing mathematical models like quantitative structure-property relationship (QSPR) and quantitative structure-activity relationship (QSAR) models. These models utilize topological indices (TI) to predict various physical and chemical properties associated with drugs. Todeschini and Consonni [33] described the formulation of a QSPR model as follows:

$$P = f(x_1, x_2, ..., x_n), \tag{1}$$

where P is the physicochemical property, $x_1, x_2, ..., x_n$ is the TI considered, and f is a function that represents the relationship between the physicochemical properties and TIs. In many cases, the specific form of f is unknown and needs to be estimated. Multiple linear regression (ordinary least squares) is often used to estimate the relationship between TIs and physicochemical properties. Alternatively, partial least squares regression can handle a large amount of data relative to the number of training compounds. When the relationship between TIs and physicochemical properties is nonlinear, other regression techniques such as artificial neural networks in QSAR and support vector regression are employed. These models combine TI and regression algorithms to predict the physicochemical properties of drugs or chemical compounds. They provide a computational approach to forecast the properties and behaviours of potential drug candidates, offering valuable assistance in laboratory drug design and reducing the reliance on costly and time-consuming experimental processes. (See [3,26,32,44,46].)

The history of TI will be incomplete without the works of Harold Wiener who introduced the first index known as Wiener index [40] in 1947. The Wiener index is a distance-based index defined as the sum of the lengths of the shortest paths between all pairs of vertices in a chemical graph representing the non-hydrogen atoms in the molecule. The index studied the molecular branching of paraffin molecules and also correlated some physicochemical properties of paraffin molecules, it was later concluded that the Wiener index is not suitable for modelling large and complex compounds, this gave room for introduction of subsequent TIs. In 1972, the first vertex-degree-based TI was introduced by Trinajstic and Gutman [20], this group of TI was known as the Zagreb indices (first and second Zagreb index), they examined the dependence of the indices on the total π-electron energy on molecular structures, it was observed that the Zagreb indices reflected the extent of branching of the molecular skeleton (see [21,31]). Later, Milan Randić introduced another degree-based index called the Randić index [35], it is also known as the connectivity index before it was renamed after Milan Randić. Initially, the Randić index did not attract much attention from researchers within the first two decades of its existence because it was considered too simple but in 1998 Bollobas and Erdos [11] studied the generalized case of the Randić index called the α-weights. The bounds of this extremal weights were studied on various graphs, theoretical results obtained from the bounds of the studied graphs gave subsequent researchers the idea to extend the Randić index to higher molecular graphs. Today the Randić index is the most studied TI and one of the most effective TI used for predictions of physicochemical properties of compounds.

The atom bond connectivity (ABC) index was conceived by Estrada et al. [15] in 1998. The ABC index is a vertex degree-based index used to describe the heat of formation of alkanes, the advantage of the ABC index over the earlier indices is that it pays more attention to small structural modifications of molecules, this means that little changes can lead to changes in the value of the ABC index although the limitation of the ABC index is that, it does not reflect the extent of branching of molecules. Recently in 2009, Vukičević and Furtula [39] introduced the vertex degree-based index of geometric-arithmetic (GA) index, this index was conceived from the geometric and arithmetic means inequality. The GA index has computational advantage in QSPR modelling process. Adnan et al. [3] studied the QSPR analysis of eight physical properties of antituberculosis drugs using different degree-based TI (Zagreb indices, forgotten index, ABC index, GA index etc) and linear regression model, his analysis showed that the topological indices correlated well with six out of eight physical properties of antituberculosis drugs studied, although two physical properties failed to correlate with any of the TI. (See [14,24,30] for more applications on TI.)

Presently, degree-based TI are being modified to obtain a more efficient index called neighbourhood degree-based TI, this TI is computed by summing the degree of neighbours of a vertex. The neighbourhood degree-based TI plays an important role in addressing some of the shortcomings of the degree-based TI such as limited applicability to larger molecules and inability to capture enough information about gradual changes in the changes of structures of a molecule. The idea of neighbourhood degree-based TI was conceived by Mondal et al. [29] in 2019. They first extended the idea of neighbourhood degree-based TI over the following set of degree-based TI; forgotten index, first Zagreb index, second Zagreb index and hyper Zagreb index. To determine the strength and efficiency of the neighbourhood degree-based TI against the degree-based TI, QSPR analysis was conducted using linear regression and the results showed that the predictive ability of neighbourhood degree-based TI performed better in application compared to degree-based TI when it was applied to study the physicochemical properties of octane isomers. In 2021, Mondal et al. in [28] further extended the concept of neighbourhood degree-based TI over another class of degree-based TI such as Randić index, inverse Randić index, sum connectivity index, redefined third Zagreb index, symmetric division degree index and applied it to the QSPR analysis of octane isomers using linear regression model. They [28] concluded that the predictive ability of the neighbourhood degree-based TI is much stronger because the correlations between these neighbourhood degree-based TI and the different properties and activities of octane isomers are very much strong. In addition, Abubakar et al. [1] also investigated the bounds of the neighbourhood versions of the degree-based geometric-arithmetic index and atom bond connectivity index over a class of graphs with fixed number of vertices including the irregular and pendant graphs. Generally, the neighbourhood degree-based TI takes into account certain features of a graph that enables its robustness and applicability in QSPR modelling, for example, it takes into consideration the entire shape of a graph and changes gradually as the graph changes in pattern, it is also easily applicable to larger molecules, neighbourhood degree-based TI can further give information about molecular symmetry and local structural features of a molecule. Predictions of physicochemical properties of molecules and compounds are dependent upon the combination of a TI and the machine learning algorithm, this combination will determine how well the algorithm will predict the physicochemical properties. In order to gain insight into the efficiency of neighbourhood degree-based TI and its applications to drug property-relationships, we are motivated to achieve the following objectives:

(1) Computation of neighbourhood degree-based TI of 15 antituberculosis drugs.
(2) QSPR analysis of the neighbourhood degree-based TI using an efficient and flexible machine learning algorithm.
(3) Comparative analysis of the efficiency of machine learning algorithms.

This paper is outlined as follows. In Section 2, we review some materials and method about neighbourhood degree-based TI and the regression models used in this paper. In Section 3, we present the dataset used for the QSPR analysis and further present the result of the regression models. Section 4 reports the experimental results of our QSPR analysis and also displays the plots of our QSPR model. Section 5 concludes this paper.

2. Materials and method

A graph $\mathcal{G}$ consists of a finite nonempty set V of objects called vertices and a set $E(\mathcal{G})$ of unordered pairs called edges [12]. The graphs considered in this work are simple, undirected and connected graphs. The neighbour degree of a vertex v denoted by δ_v is defined as the sum of the degrees of the neighbours of v, this is given by

$$\delta_v = \sum_{u \in N(v)} d_u, \tag{2}$$

where $N(v)$ is the neighbours of vertex v. The neighbourhood topological indices considered in this work are given below:

i. Neighbourhood geometric-arithmetic index [1]

$$NGA(\mathcal{G}) = \sum_{u,v \in E(\mathcal{G})} \frac{2\sqrt{\delta_u \delta_v}}{\delta_u + \delta_v}. \tag{3}$$

ii. Neighbourhood atom bond connectivity index [1]

$$NABC(\mathcal{G}) = \sum_{u,v \in E(\mathcal{G})} \sqrt{\frac{\delta_u + \delta_v - 2}{\delta_u \delta_v}}. \tag{4}$$

iii. Neighbourhood first Zagreb index [29] is given by

$$NM_1(\mathcal{G}) = \sum_{u,v \in E(\mathcal{G})} [\delta_u + \delta_v]. \tag{5}$$

iv. Neighbourhood version of second Zagreb index [29] is given by

$$NM_2(\mathcal{G}) = \sum_{u,v \in E(\mathcal{G})} [\delta_u \delta_v]. \tag{6}$$

v. Neighbourhood version of Randić index [28] is given by

$$NR(\mathcal{G}) = \sum_{u,v \in E(\mathcal{G})} \frac{1}{\sqrt{\delta_u \delta_v}}. \tag{7}$$

vi. Neighbourhood version of inverse Randić index [28] is given by

$$NRR(\mathcal{G}) = \sum_{u,v \in E(\mathcal{G})} \sqrt{\delta_u \delta_v}. \tag{8}$$

vii. Neighbourhood version of hyper Zagreb index [29] is given by

$$NHP(\mathcal{G}) = \sum_{u,v \in E(\mathcal{G})} [\delta_u + \delta_v]^2. \tag{9}$$

viii. Neighbourhood version of harmonic index [28] is given by

$$NHM(\mathcal{G}) = \sum_{u,v \in E(\mathcal{G})} \frac{2}{\delta_u + \delta_v}. \tag{10}$$

2.1. Dataset acquisition

In this work, fifteen neighbourhood degree based TI for antituberculosis drugs were computed and used to evaluate the performance of SVR model while benchmarking with LR model in the QSPR analysis of eight physical properties of antituberculosis drugs. Antituberculosis drugs have different physical properties depending on the drug been studied, for example, amikacin is a white cream-coloured powder at room temperature with a molecular weight of approximately $585.6g \setminus mol$ and a melting point of over $200\,^{\circ}C$, it is also an odorless substance, isoniazid has a melting point of $172\,^{\circ}C$ while pyrazinamide has a melting point of $190\,^{\circ}C$. In general, antituberculosis drugs can be unstable and may degrade over time, factors such as temperature and humidity can affect their stability. For brevity, we considered only eight physical properties of fifteen antituberculosis drugs in this work which have been presented in Table 1, this includes boiling point (Bp), melting point (Mp), flash point (Fp), enthalpy of vaporization (Ev), molar refraction (MR), polarization (P), surface tension (ST) and molar volume (Mv). The dataset for the physical properties was obtained from Chemspider (www.chemspider.com), missing data from the physical properties was computed using their median values. The molecular structures of antituberculosis drugs have been displayed in section 3. The dataset in Table 3 was derived by computing the neighbourhood degree-based topological index of each of the molecular structures using (3)-(10).

2.2. The SVR theory

One of the most efficient algorithm that can be combined with a TI to obtain efficient prediction is the support vector regression (SVR), this is a variant of the support vector machine (SVM), it is used purposely for solving regression problems. The SVR is an efficient ML algorithm that is known for its use of support vectors to find a hyperplane that best fits the data while minimizing the margin. Although most QSPR analysis in past literature [3,35,34,36] used LR model in the QSPR of physicochemical properties of compounds, this is because the LR model is simple, easy to understand and has interpretable coefficient of correlation. The disadvantages are quite numerous especially when compared to the SVR. SVR can capture nonlinear relationships between data and is less sensitive to outliers in the data compared to LR. SVR focuses on capturing the overall trend of the data while disregarding individual data points that deviate significantly, leading to more improved and better predictions. It also allows the use of various kernel functions, such as linear, polynomial, radial basis function (RBF), or sigmoid kernels. This flexibility enables the modelling of different data patterns and can improve prediction accuracy compared to LR. Furthermore, SVR can implicitly perform feature selection by selecting a subset of relevant features or variables from a larger set of available features in a dataset improving the model's generalization and effectively handling high-dimensional data (see [2,9,10,23] for more details on machine learning). These combined advantages make SVR a powerful regression technique, capable of modelling complex patterns, improving prediction accuracy, and offering robustness in various domains such as genomics, bioinformatics, and QSPR (see [16,17,24,41]). Due to these

advantages of the SVR, Yang et al. [41] used support vector regression (SVR) integrated with TI to predict the physicochemical properties of alkyl benzene, SVR was used to separate pure components from alkyl benzene mixture, in a benchmark test, the SVR model was compared with several modelling technique such as the back propagation artificial neural network (BP ANN) and partial least square (PLS) method, the SVR performed better than the other models adopted. (See [42,45] for further applications of the SVR in QSPR analysis.) The parameters used to determine the efficiency of the regression models are defined below:

Definition 2.1. [9,43] Let y be a dependent variable (target feature) on the set of independent variables (input feature) $x = (x_1, x_2, ..., x_r)$ where r is the number of predictors, a linear regression between y and x is defined as

$$y = c + b_1 x_1 + ... + b_r x_r + \epsilon, \tag{11}$$

where $c, b_1, ..., b_r$ are the regression coefficients and ϵ is the random error. A QSPR model is built using the following LR model;

$$P = c + b(TI), \tag{12}$$

where $y = P$, and P is the physicochemical property (dependent variable) of the chemical compound, c is the intercept of regression, b is the regression coefficients and TI represents the topological index (independent variable).

Definition 2.2. [9,41] Let x_i be an independent variable, F a higher dimensional feature space via a nonlinear mapping $f(x)$, an SVR is defined over the space F as

$$y = f(x_1, x_2, ..., x_n) = < w, x_i > + b = \sum_{i=1}^{n} w \cdot x_i + b, \tag{13}$$

for $y, b \in \mathbb{R}, x_i, w \in \mathbb{R}^M$ where x_i is the set of mappings of input features; w and b are the regression coefficients. If the data is non-linear with kernel function radial basis function (RBF), this is evaluated with the equation

$$y = f(x_1, x_2, ..., x_n) = \sum_{i=1}^{n} \alpha_i \cdot K(x_i, x') + b, \tag{14}$$

where α_i represent the Langrange multipliers obtained during the model training process, $K(x_i, x')$ is the RBF kernel function applied to the input feature x_i and support vectors x'.

Definition 2.3. The RBF kernel is a kernel function used to transform data into a higher dimensional space, it is defined by the equation

$$K(x_i, x') = exp\left(-\frac{||x_i - x'||^2}{2\sigma^2}\right), \tag{15}$$

where $||x - x'||^2$ is the squared Euclidean distance between the feature vectors x_i and x' and σ is a free parameter. For γ parameter, the RBF kernel becomes

$$K(x_i, x') = exp(-\gamma ||x - x'||^2), \tag{16}$$

where $\gamma = \frac{1}{2\sigma^2}$.

Next, the parameters used to determine the efficiency of the regression models are defined below:

Definition 2.4. [41,43] Root mean squared error (RMSE) is the square root of the difference between the actual and predicted values extracted by squaring the average difference over the dataset. It is given by the equation

$$RMSE = \sqrt{\frac{1}{N}\sum_{i=1}^{N}(y_i - \hat{y})^2}, \tag{17}$$

where y is the experimental sample, $\hat{y}$ is the predicted value and N is the number of all the samples in the cross validation.

Definition 2.5. Regularization (cost) parameter (C) is a regression parameter that constrains or shrinks the estimates of coefficients of regression towards zero so as to avoid overfitting the model.

2.3. Perfomance assessment

Two regression variables will be used for the SVR and LR implementation namely; independent variable or input feature will consist of computed neighbourhood degree-based TI of antituberculosis drugs while dependent variable or target feature will consist of the physical properties of antituberculosis drugs. To determine the efficiency of SVR, we will compare the SVR with LR to

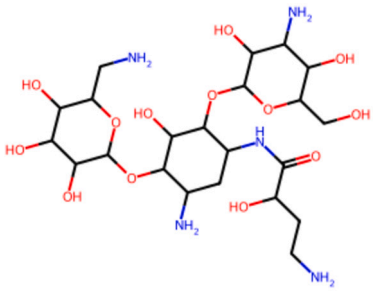

Fig. 1. Amikacin.

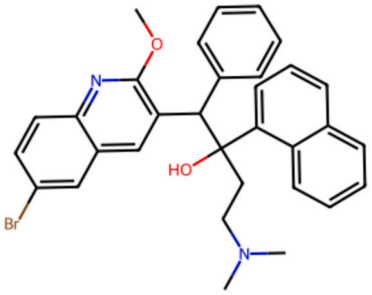

Fig. 2. Bedaquiline.

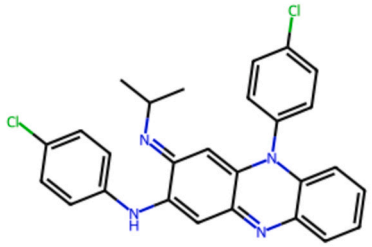

Fig. 3. Clofazimine.

determine which of the models have a better predictive ability (lower RMSE value). The regression performance of LR and SVR will be determined by a cross validation method called Leave-one-out cross validation (LOOCV), we will introduce this for our parameter selection. This validation helps evade the chances of high variance that is usually recorded in the train-split method when the dataset is small. LOOCV is done by picking one sample as a test set while the rest are used to train our model, this will be done by dividing the dataset into two disjoint subsets which includes the training data set of $n-1$ samples and a test data set of 1 sample. After developing each model based on the training set, the omitted data will be predicted and the difference between the experimental/actual value and predicted value will be computed. The average root mean squared error (RMSE) across the LOOCV will be adopted as a criterion of optimal set for the SVR model, the RMSE will also be adopted for the LR model in our QSPR analysis. Better efficiency is determined by the least possible value of RMSE obtainable, this describes the efficiency of the model. The performance of SVR model is determined by the combination of parameters used in the regression, the following parameters have been selected for the regression model: Regularization parameter C and γ value of radial basis function (RBF). The C parameter will be optimized together with the RBF γ value using the grid search method. The implementation environment for the LR and SVR is python (pycharm software).

3. Results and discussion

In this section, we present the molecular structures and chemical graphs of fifteen antituberculosis drugs. The fifteen drugs considered are: Amikacin 1, Bedaquiline 2, Clofazimine 3, Delamanid 4, Ethambutol 5, Ethionamide 6, Imipenem 7, Isoniazid 8, Levofloxacin 9, Linezolid 10, Moxifloxacin 11, 4-Aminosalicylic acid 12, Pyrazinamide 13, Rifampicin 14, and Terizidone 15.

Molecular compounds are known to posses physical properties, a compound's physical property is any property that is a measurable and observable. Table 1 presents the physical properties of antituberculosis drugs that will be considered in this research such as boiling point (Bp), melting point(Mp), flash point (Fp), enthalpy of vapourization (Ev), molar refraction (MR), surface tension

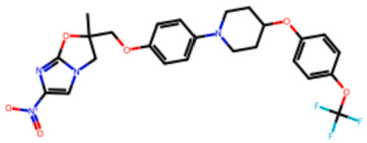

Fig. 4. Delamanid.

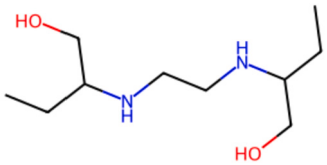

Fig. 5. Ethambutol.

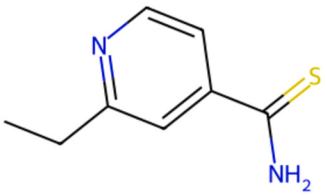

Fig. 6. Ethionamide.

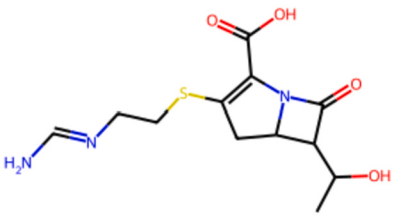

Fig. 7. Imipenem.

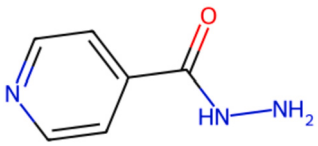

Fig. 8. Isoniazid.

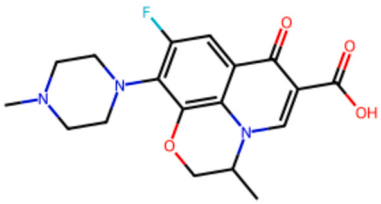

Fig. 9. Levofloxacin.

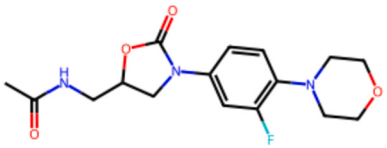

Fig. 10. Linezolid.

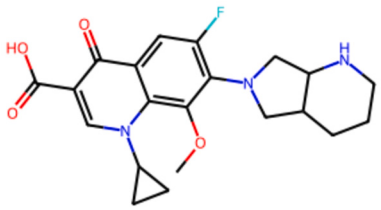

Fig. 11. Moxifloxacin.

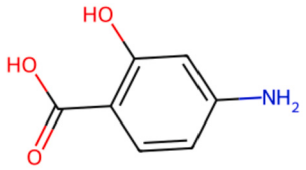

Fig. 12. 4-Aminosalicylic acid.

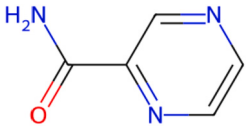

Fig. 13. Pyrazinamide.

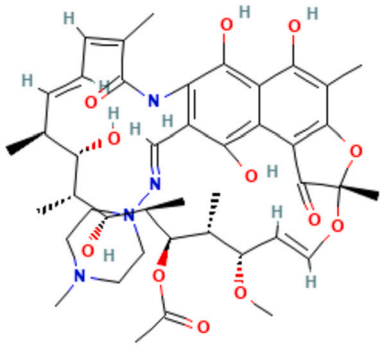

Fig. 14. Rifampicin.

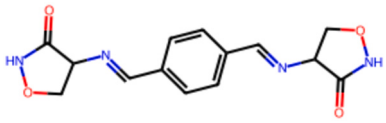

Fig. 15. Terizidone.

(ST), polarization (P) and molar volume (Mv). The dataset for physical properties of antituberculosis drugs represents our target or dependent variable in the model.

To obtain the dataset for our input or independent feature, we illustrate computation of neighbourhood degree-based TI using the chemical graph of terizidone. The labelling on the edges indicates the neighbours degrees of the vertices. For example, edge label m_2 indicates vertices with neighbours degrees 4 and 5, edge label m_4 indicates vertices with neighbours degree 5 and 6. The vertex labelling on the other hand indicates the degree of each vertex in the chemical graph. The computed neighbourhood index values are presented in Table 3. (See [8] for chemical graphs of antituberculosis drugs.)

Proposition 3.1. *Let $\mathcal{G}$ be a chemical graph of terizidone (see Fig. 16) with* 24 *edges, then*

(i) $NM1(\mathcal{G}) = 256$
(ii) $NM2(\mathcal{G}) = 680$

Table 1
Physical properties of antituberculosis drugs obtained from ChemSpider.

Medicine	Bp	Mp	Fp	Ev	MR	P	ST	Mv
Amikacin	981.8	203.5	547.6	162.2	134.9	53.5	103.3	363.9
Bedaquiline	702.7	176	378.8	108	156.2	61.9	52.6	420.1
Clofazimine	566.9	210	296.7	85.1	136.2	54	47.1	366.1
Delamanid	653.7	193	349.1	96.3	127.7	50.6	50	368
Ethambutol	345.3	89	113.7	68.3	58.6	23.2	38.1	207
Ethionamide	247.9	163	103.7	46.5	49	19.4	39.8	142
Imipenem	530.2	-	274.5	92.7	72.7	28.8	71	183.9
Isoniazid	251.97	172	251	-	36.9	14.6	57.8	110.2
Levofloxacin	571.5	224	299.4	90.1	91.1	36.1	70.3	244
Linezolid	585.5	177	307.9	87.5	83	32.9	47.7	259
Moxifloxacin	636	270	338.7	98.8	101.8	40.4	60.6	285
4-Aminosalicyclic acid	380.8	145	184.1	66.3	39.3	15.6	83.4	102.7
Pyrazinamide	173.3	190	119.1	54.1	31.9	12.6	60.7	87.7
Rifampin	937.4	183	561.3	153.5	213.1	84.5	48	611.7
Terizidone	-	175	-	-	76.1	30.2	62.5	198.9

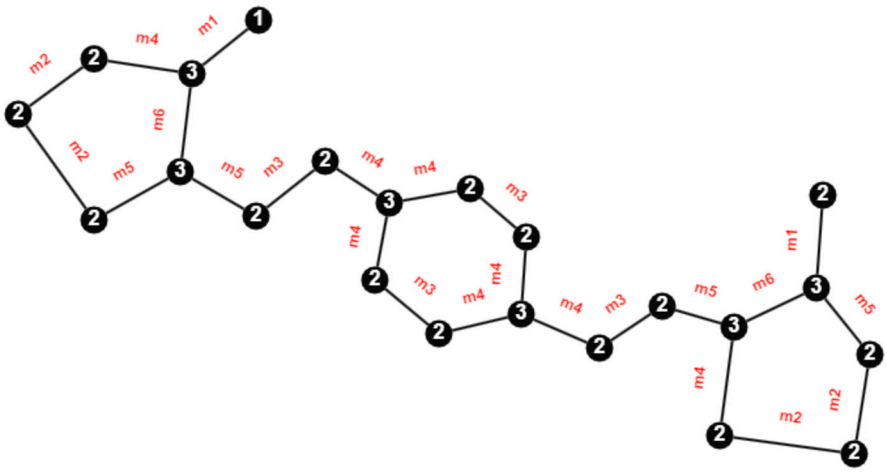

Fig. 16. Chemical graph of terizidone.

Table 2
Edge partition set of terizidone chemical graph.

Edge label	$\delta(u,v)$	Number of edges (m)
m_1	$(3,6)$	2
m_2	$(4,5)$	4
m_3	$(5,5)$	4
m_4	$(5,6)$	8
m_5	$(5,7)$	4
m_6	$(6,7)$	2

(iii) $NHP(\mathcal{G}) = 2768$
(iv) $NHM(\mathcal{G}) = 4.56$
(v) $NR(\mathcal{G}) = 4.61$
(vi) $NRR(\mathcal{G}) = 126.82$
(vii) $NGA(\mathcal{G}) = 23.765$
(viii) $NABC(\mathcal{G}) = 13.42.$

Proof. We partition the edge set of terizidone chemical graph via sum of degrees of neighbours of vertices as follows in Table 2 and thus establish our proof.

(i) For neighbourhood first Zagreb index

$$NM1(\mathcal{G}) = \sum_{uv \in E(\mathcal{G})} (\delta_u + \delta_v) = m_1(\delta_3 + \delta_6) + m_2(\delta_4 + \delta_5) + m_3(\delta_5 + \delta_5)$$

$$+ m_4(\delta_5+\delta_6) + m_5(\delta_5+\delta_7) + m_6(\delta_6+\delta_7)$$
$$= 2(9) + 4(9) + 4(10) + 8(11) + 4(12) + 2(13)$$
$$= 256.$$

(ii) For neighbourhood second Zagreb index

$$NM2(\mathcal{G}) = \sum_{uv\in E(\mathcal{G})} (\delta_u\delta_v) = m_1(\delta_3\delta_6) + m_2(\delta_4\delta_5) + m_3(\delta_5\delta_5)$$
$$+ m_4(\delta_5\delta_6) + m_5(\delta_5\delta_7) + m_6(\delta_6\delta_7)$$
$$= 2(18) + 4(20) + 4(25) + 8(30) + 4(35) + 2(42)$$
$$= 680.$$

(iii) For neighbourhood Hyper Zagreb index

$$NHP(\mathcal{G}) = \sum_{uv\in E(\mathcal{G})} (\delta_u+\delta_v)^2 = m_1(\delta_3+\delta_6)^2 + m_2(\delta_4+\delta_5)^2 + m_3(\delta_5+\delta_5)^2$$
$$+ m_4(\delta_5+\delta_6)^2 + m_5(\delta_5+\delta_7)^2 + m_6(\delta_6+\delta_7)^2$$
$$= 2(81) + 4(81) + 4(100) + 8(121) + 4(144) + 2(169)$$
$$= 2768.$$

(iv) For neighbourhood harmonic index

$$NHM(\mathcal{G}) = \sum_{uv\in E(\mathcal{G})} \frac{2}{\delta_u+\delta_v} = m_1\left(\frac{2}{\delta_3+\delta_6}\right) + m_2\left(\frac{2}{\delta_4+\delta_5}\right) + m_3\left(\frac{2}{\delta_5+\delta_5}\right)$$
$$+ m_4\left(\frac{2}{\delta_5+\delta_6}\right) + m_5\left(\frac{2}{\delta_5+\delta_7}\right) + m_6\left(\frac{2}{\delta_6+\delta_7}\right)$$
$$= 2\left(\frac{2}{9}\right) + 4\left(\frac{2}{9}\right) + 4\left(\frac{2}{10}\right) + 8\left(\frac{2}{11}\right) + 4\left(\frac{2}{12}\right) + 2\left(\frac{2}{13}\right)$$
$$= 4.562.$$

(v) For neighbourhood Randić index

$$NR(\mathcal{G}) = \sum_{uv\in E(\mathcal{G})} \frac{1}{\sqrt{\delta_u\delta_v}} = m_1\left(\frac{1}{\sqrt{\delta_3\delta_6}}\right) + m_2\left(\frac{1}{\sqrt{\delta_4\delta_5}}\right) + m_3\left(\frac{1}{\sqrt{\delta_5\delta_5}}\right)$$
$$+ m_4\left(\frac{1}{\sqrt{\delta_5\delta_6}}\right) + m_5\left(\frac{1}{\sqrt{\delta_5\delta_7}}\right) + m_6\left(\frac{1}{\sqrt{\delta_6\delta_7}}\right)$$
$$= 2\left(\frac{1}{\sqrt{18}}\right) + 4\left(\frac{1}{\sqrt{20}}\right) + 4\left(\frac{1}{5}\right) + 8\left(\frac{1}{\sqrt{30}}\right) + 4\left(\frac{1}{\sqrt{35}}\right) + 2\left(\frac{1}{\sqrt{42}}\right)$$
$$= 4.611.$$

(vi) For neighbourhood reciprocal Randić index

$$NRR(\mathcal{G}) = \sum_{uv\in E(\mathcal{G})} \sqrt{\delta_u\delta_v} = m_1(\sqrt{\delta_3\delta_6}) + m_2(\sqrt{\delta_4\delta_5}) + m_3(\sqrt{\delta_5\delta_5})$$
$$+ m_4(\sqrt{\delta_5\delta_6}) + m_5(\sqrt{\delta_5\delta_7}) + m_6(\sqrt{\delta_6\delta_7})$$
$$= 2(\sqrt{18}) + 4(\sqrt{20}) + 4(5) + 8(\sqrt{30}) + 4(\sqrt{35}) + 2(\sqrt{42})$$
$$= 126.82.$$

(vii) For neighbourhood geometric-arithmetic index

$$NGA(\mathcal{G}) = \sum_{uv\in E(\mathcal{G})} \frac{2\sqrt{\delta_u\delta_v}}{\delta_u+\delta_v} = m_1\left(\frac{2\sqrt{\delta_3\delta_6}}{\delta_3+\delta_6}\right) + m_2\left(\frac{2\sqrt{\delta_4\delta_5}}{\delta_4+\delta_5}\right) + m_3\left(\frac{2\sqrt{\delta_5\delta_5}}{\delta_5+\delta_5}\right)$$
$$+ m_4\left(\frac{2\sqrt{\delta_5\delta_6}}{\delta_5+\delta_6}\right) + m_5\left(\frac{2\sqrt{\delta_5\delta_7}}{\delta_5+\delta_7}\right) + m_6\left(\frac{2\sqrt{\delta_6\delta_7}}{\delta_6+\delta_7}\right)$$

Table 3
Neighbourhood topological indices of antituberculosis drugs.

Medicine	NGA($\mathcal{G}$)	NABC($\mathcal{G}$)	$NM1(\mathcal{G})$	$NM2(\mathcal{G})$	NR($\mathcal{G}$)	NRR($\mathcal{G}$)	NHP($\mathcal{G}$)	NHM($\mathcal{G}$)
Amikacin	40.96	23.25	491	1455	7.92	240.55	6200	7.68
Bedaquiline	40.52	22.43	481	1488	7.63	237.8	6081	7.57
Clofazimine	38.76	20.19	425	1272	6.87	211.25	5145	6.82
Delamanid	41.71	23.28	481	1389	7.55	238.98	5621	7.49
Ethambutol	12.66	9.91	112	244	3.29	54.81	1012	3.19
Ethionamide	10.81	6.39	110	280	2.36	54.21	1148	2.31
Imipenem	22.32	11.85	286	1022	3.57	138.91	4298	3.45
Isoniazid	9.8	6.11	87	192	2.48	42.65	799	2.43
Levofloxacin	27.53	15.02	341	1072	4.99	168.01	4401	4.89
Linezolid	25.73	14.43	288	819	4.99	142.62	3226	4.93
Moxifloxacin	31.36	17.13	424	1417	10.14	208.13	5854	5.08
4-Aminosalicyclic-acid	10.76	6.65	109	277	2.46	53.37	1153	2.41
Pyrazinamide	8.89	5.28	86	207	1.97	42.44	850	1.94
Rifampin	60.55	32.84	742	2286	11.41	363.67	9438	11.09
Terizidone	23.77	13.42	256	680	4.61	126.82	2768	4.56

$$= 2\left(\frac{2\sqrt{18}}{9}\right) + 4\left(\frac{2\sqrt{20}}{9}\right) + 4\left(\frac{2\sqrt{25}}{10}\right) + 8\left(\frac{2\sqrt{30}}{11}\right) + 4\left(\frac{2\sqrt{35}}{12}\right) + 2\left(\frac{2\sqrt{42}}{13}\right) = 23.77.$$

(viii) For neighbourhood atom bond connectivity index

$$NABC(\mathcal{G}) = \sum_{uv\in E(\mathcal{G})}\sqrt{\frac{\delta_u+\delta_v-2}{\delta_u\delta_v}} = m_1\left(\sqrt{\frac{\delta_3+\delta_6-2}{\delta_3\delta_6}}\right) + m_2\left(\sqrt{\frac{\delta_4+\delta_5-2}{\delta_4\delta_5}}\right) + m_3\left(\sqrt{\frac{\delta_5+\delta_5-2}{\delta_5\delta_5}}\right) + m_4\left(\sqrt{\frac{\delta_5+\delta_6-2}{\delta_5\delta_6}}\right) + m_5\left(\sqrt{\frac{\delta_5+\delta_7-2}{\delta_5\delta_7}}\right) + m_6\left(\sqrt{\frac{\delta_6+\delta_7-2}{\delta_6\delta_7}}\right).$$

$$= 2\left(\sqrt{\frac{7}{18}}\right) + 4\left(\sqrt{\frac{7}{20}}\right) + 4\left(\sqrt{\frac{8}{25}}\right) + 8\left(\sqrt{\frac{9}{30}}\right) + 4\left(\sqrt{\frac{10}{35}}\right) + 2\left(\sqrt{\frac{11}{42}}\right).$$

$$= 13.42. \quad \square$$

Remark 3.2. The neighbourhood degree-based TI of 14 other antituberculosis drugs were computed via the same method as Proposition 3.1.

The Table below displays computed data for neighbourhood degree-based TI.

4. Model implementation and experimental results

From Table 1 and Table 3, we implement a QSPR model using (1) to predict the physical properties of antituberculosis drugs. Two regression algorithms, SVR and LR models are utilized in our QSPR model of the physical properties of antituberculosis drugs. The LR model was implemented using (11) while the SVR model was implemented using (14). The LOOCV was chosen for the SVR, this is demonstrated in the following algorithm below. In this context, x refers to the input feature, which consists of neighbourhood degree-based TIs, and y represents the target feature, which corresponds to the physical properties we aim to predict.

Tables 4 - 19 display the experimental results from the implemented QSPR model. The table includes the predicted values from the SVR and LR models and their respective physical property.

4.1. Evaluation of model performance

To evaluate the efficacy of the experimental results shown in Table 4 to Table 19, we examine the performance metrics of SVR and LR, as described in Tables 20 to 27. The effectiveness of a model is determined by its ability to demonstrate lower RMSE values for each physical property.

Table 4
Experimental and actual data for prediction of NGA and physical properties of antituberculosis drugs.

Medicine	Pred. (LR1)	Pred. (SVR1)	Bp	Pred. (LR2)	Pred. (SVR2)	Mp	Pred. (LR3)	Pred. (SVR3)	Fp	LR4	SVR4	Ev
Amikacin	736.49	707.29	981.8	197.92	194.95	203.5	405.91	379.02	547.6	116.07	108.69	162.2
Bedaquiline	730.33	728.45	702.7	197.45	198.97	176	402.39	377.68	378.8	115.34	109.35	108
Clofazimine	705.69	702.98	566.9	195.58	194.55	210	388.32	369.06	296.7	112.40	106.70	85.1
Delamanid	746.99	741.97	653.7	198.71	203.36	193	411.91	387.52	349.1	117.32	111.16	96.3
Ethambutol	340.33	401.78	345.3	167.85	155.28	89	179.67	221.83	113.7	68.86	70.15	68.3
Ethionamide	314.44	381.44	247.9	165.89	143.66	163	164.89	212.59	103.7	65.79	68.02	46.5
Imipenem	475.56	504.80	530.2	178.12	158.95	177	256.90	267.03	274.5	84.97	82.49	92.7
Isoniazid	300.30	370.49	251.97	164.82	168.59	172	156.81	188.53	251	64.08	65.02	92.1
Levofloxacin	548.49	562.28	571.5	183.65	197.22	224	298.55	304.56	299.4	93.67	89.96	90.1
Linezolid	523.29	542.36	585.5	181.74	200.75	177	284.16	288.40	307.9	90.66	87.42	87.5
Moxifloxacin	602.10	604.63	636.0	187.72	263.18	270	329.17	323.10	338.7	100.06	95.38	98.8
4-Aminosalicyclic acid	341.51	380.8	165.84	187.72	152.37	145	164.49	212.35	184.1	65.68	68.01	66.3
Pyrazinamide	287.56	360.73	173.3	163.85	196.09	190	149.54	203.44	119.1	62.56	66.40	54.1
Rifampin	1010.72	856.12	937.4	218.73	193.55	183	562.52	428.23	561.3	148.76	126.18	153.5
Terizidone	495.86	520.73	566.9	179.66	185.64	175	268.49	276.01	298.1	87.39	84.58	92.1

Table 5
(Cont'd) experimental and actual data for prediction of NGA and physical properties of antituberculosis drugs.

Medicine	Pred. (LR5)	Pred. (SVR5)	MR	Pred. (LR6)	Pred. (SVR6)	P	Pred. (LR7)	Pred. (SVR7)	ST	Pred. LR8	Pred. (SVR8)	Mv
Amikacin	139.96	139.26	134.9	55.49	55.23	53.5	59.76	50.39	103.3	390.12	372.09	363.9
Bedaquiline	138.50	134.15	156.2	54.91	53.86	61.9	59.75	50.55	52.6	386.10	360.01	420.1
Clofazimine	132.66	128.14	136.2	52.59	51.23	54.0	59.72	53.84	47.1	370.03	344.89	366.1
Delamanid	142.44	142.12	127.7	56.48	56.36	50.6	59.77	52.50	50.0	396.97	379.20	368.0
Ethambutol	46.08	44.02	58.6	18.25	17.43	23.2	59.29	58.38	38.1	131.73	130.24	207.0
Ethionamide	39.95	39.34	49	15.82	15.55	19.4	59.26	57.76	39.8	114.83	117.14	142.0
Imipenem	78.13	72.02	72.7	30.96	28.61	28.8	59.45	61.42	71.0	219.93	207.90	183.9
Isoniazid	36.60	37.01	36.9	14.49	14.77	14.6	59.24	57.54	57.8	105.61	119.04	110.2
Levofloxacin	95.41	89.17	91.1	37.82	35.28	36.1	59.53	62.52	70.3	267.50	251.79	244.0
Linezolid	89.44	84.01	83	35.45	33.34	32.9	59.50	63.29	47.7	251.06	231.63	259.0
Moxifloxacin	108.11	103.61	101.8	42.86	41.10	40.4	59.59	58.45	60.6	302.47	279.85	285.0
4-Aminosalicyclic acid	39.78	39.39	39.3	15.75	15.64	15.6	59.25	57.25	83.4	114.38	120.99	102.7
Pyrazinamide	33.58	34.81	31.9	13.29	13.93	12.6	60.08	57.61	60.7	97.30	117.36	87.7
Rifampin	204.94	197.65	213.1	81.26	78.52	84.5	59.47	57.79	48.0	568.99	499.65	611.7
Terizidone	82.94	77.50	76.1	32.87	30.76	30.2	59.47	63.38	62.5	233.17	219.98	198.9

Table 6
Experimental and actual data for prediction of NABC and physical properties of antituberculosis drugs.

Medicine	Pred. (LR1)	Pred. (SVR1)	Bp	Pred. (LR2)	Pred. (SVR2)	Mp	Pred. (LR3)	Pred. (SVR3)	Fp	LR4	SVR4	Ev
Amikacin	758.96	704.01	981.8	197.21	192.21	203.5	417.55	384.57	547.6	118.97	110.20	162.2
Bedaquiline	736.96	695.58	702.7	195.78	200.96	176	405.10	379.11	378.8	116.32	111.99	108
Clofazimine	676.87	674.59	566.9	191.89	169.06	210	371.09	356.93	296.7	109.09	105.33	85.1
Delamanid	759.76	716.53	653.7	197.26	204.48	193	418.01	395.45	349.1	119.06	114.55	96.3
Ethambutol	401.10	428.58	345.3	174.02	151.94	89	215.01	242.76	113.7	75.93	75.96	68.3
Ethionamide	306.68	264.24	247.9	167.90	158.93	163	161.57	179.79	103.7	64.57	69.37	46.5
Imipenem	453.15	471.32	530.2	177.39	177.32	177	244.46	273.12	274.5	82.19	80.36	92.7
Isoniazid	299.17	235.55	251.97	167.42	168.84	172	157.31	136.43	251	63.67	64.75	92.1
Levofloxacin	538.18	598.97	571.5	182.90	196.94	224	292.60	314.13	299.4	92.41	89.01	90.1
Linezolid	522.36	556.29	585.5	181.88	199.01	177	283.64	307.37	307.9	90.51	88.32	87.5
Moxifloxacin	594.78	622.01	636.0	186.57	264.84	270	324.63	328.97	338.7	99.22	94.78	98.8
4-Aminosalicyclic acid	313.65	259.41	380.8	168.35	154.17	145	165.51	147.57	184.1	65.41	69.96	66.3
Pyrazinamide	276.90	220.49	173.3	165.97	200.57	190	144.71	164.48	119.1	60.99	66.89	54.1
Rifampin	1016.21	556.18	937.4	213.87	183.26	183	563.16	374.39	561.3	85.35	83.03	153.5
Terizidone	479.43	506.78	569.2	179.09	154.96	175	259.34	288.00	298.1			92.1

Table 7
(Cont'd) experimental and actual data for prediction of NABC and physical properties of antituberculosis drugs.

Medicine	Pred. (LR5)	Pred. (SVR5)	MR	Pred. (LR6)	Pred. (SVR6)	P	Pred. (LR7)	Pred. (SVR7)	ST	Pred. (LR8)	Pred. (SVR8)	Mv
Amikacin	144.98	138.81	134.9	57.48	55.59	53.5	59.62	52.28	103.3	405.15	366.68	363.9
Bedaquiline	139.79	130.41	156.2	55.42	52.38	61.9	59.61	53.06	52.6	390.75	353.07	420.1
Clofazimine	125.63	118.28	136.2	49.80	47.29	54.0	59.58	54.12	47.1	351.43	323.57	366.1
Delamanid	145.17	138.99	127.7	57.55	55.66	50.6	59.62	52.64	50.0	405.68	364.19	368.0
Ethambutol	60.62	59.02	58.6	24.02	23.45	23.2	59.46	58.63	38.1	170.96	187.64	207.0
Ethionamide	38.36	38.41	49	15.19	15.14	19.4	59.42	60.30	39.8	109.16	147.83	142.0
Imipenem	72.89	70.29	72.7	28.89	27.83	28.8	59.48	56.76	71.0	205.01	216.31	183.9
Isoniazid	36.59	37.16	36.9	14.49	14.59	14.6	59.42	60.42	57.8	104.24	144.37	110.2
Levofloxacin	92.93	88.91	91.1	36.83	35.30	36.1	59.52	55.63	70.3	260.67	256.64	244.0
Linezolid	89.20	85.67	83	35.36	34.09	32.9	59.51	56.72	47.7	250.31	247.23	259.0
Moxifloxacin	106.28	101.35	101.8	42.13	40.57	40.4	59.42	54.78	60.6	250.31	283.03	259.0
4-Aminosalicyclic acid	40.01	40.14	39.3	15.84	15.93	15.6	59.40	57.75	83.4	297.71	150.54	285.0
Pyrazinamide	31.34	34.01	31.9	12.41	12.81	12.6	59.74	57.75	60.7	113.72	134.19	102.7
Rifampin	205.62	185.31	213.1	81.53	73.69	84.5	59.50	47.89	48.0	573.51	483.00	611.7
Terizidone	79.09	76.20	76.1	31.34	30.26	30.2	59.50	56.44	62.5	222.22	228.98	198.9

Table 8
Experimental and actual data for prediction of NM1 and physical properties of antituberculosis drugs.

Medicine	Pred. (LR1)	Pred. (SVR1)	Bp	Pred. (LR2)	Pred. (SVR2)	Mp	Pred. (LR3)	Pred. (SVR3)	Fp	LR4	SVR4	Ev
Amikacin	738.23	687.57	981.8	200.15	190.24	203.5	406.91	377.01	547.6	116.32	101.40	162.2
Bedaquiline	727.12	680.17	702.7	199.20	200.73	176	400.56	372.34	378.8	114.99	101.25	108
Clofazimine	664.91	642.50	566.9	193.87	221.02	210	365.01	348.21	296.7	107.56	98.86	85.1
Delamanid	727.12	689.44	653.7	199.20	200.73	193	400.56	378.90	349.1	114.99	108.10	96.3
Ethambutol	317.22	385.07	345.3	164.09	163.03	89	166.28	185.51	113.7	66.01	66.20	68.3
Ethionamide	315.00	383.92	247.9	163.90	163.21	163	165.01	184.63	103.7	65.75	68.16	46.5
Imipenem	510.51	521.49	530.2	180.65	186.82	180	276.76	269.73	274.5	89.11	89.55	92.7
Isoniazid	289.45	370.13	251.97	161.71	168.58	172	150.41	168.35	251	62.70	63.06	92.1
Levofloxacin	571.60	567.59	571.5	185.88	195.56	224	311.67	302.63	299.4	96.41	93.29	90.1
Linezolid	512.73	523.16	585.5	180.84	188.17	177	278.02	270.80	307.9	89.38	92.55	87.5
Moxifloxacin	663.80	641.66	636.0	193.78	210.16	270	364.37	347.66	338.7	107.43	86.50	98.8
4-Aminosalicyclic acid	313.89	381.53	380.8	163.80	163.43	145	164.38	179.67	184.1	65.62	68.18	66.3
Pyrazinamide	288.34	370.87	173.3	161.61	168.66	190	149.76	175.33	119.1	62.57	75.63	54.1
Rifampin	1017.05	809.85	937.4	224.04	186.07	183	566.27	445.17	561.3	149.63	89.09	153.5
Terizidone	477.18	496.57	569.2	177.79	166.24	175	257.71	253.90	298.1	85.13	93.82	92.1

Table 9
(Cont'd) experimental and actual data for prediction of NM1 and physical properties of antituberculosis drugs.

Medicine	Pred. (LR5)	Pred. (SVR5)	MR	Pred. (LR6)	Pred. (SVR6)	P	Pred. (LR7)	Pred. (SVR7)	ST	Pred. (LR8)	Pred. (SVR8)	Mv
Amikacin	139.41	131.96	134.9	55.27	51.62	53.5	60.36	56.87	103.3	388.17	376.36	363.9
Bedaquiline	136.83	130.94	156.2	54.25	50.70	61.9	60.31	50.10	52.6	381.09	360.34	420.1
Clofazimine	122.38	111.29	136.2	48.52	45.51	54.0	60.05	61.22	47.1	341.47	322.12	366.1
Delamanid	136.83	131.17	127.7	54.25	52.41	50.6	60.31	52.70	50.0	381.09	360.34	368.0
Ethambutol	41.63	43.05	58.6	16.49	16.76	23.2	58.57	61.92	38.1	119.99	118.07	207.0
Ethionamide	41.11	42.56	49	16.28	16.58	19.4	58.56	61.79	39.8	118.57	117.00	142.0
Imipenem	86.52	81.41	72.7	34.29	33.15	28.8	59.39	59.37	71.0	243.11	222.43	183.9
Isoniazid	35.18	39.89	36.9	13.93	14.33	14.6	58.45	60.37	57.8	102.30	104.67	110.2
Levofloxacin	100.71	93.58	91.1	39.92	38.41	36.1	59.65	59.42	70.3	282.03	260.76	244.0
Linezolid	87.04	81.49	83	34.50	33.34	32.9	59.40	61.18	47.7	244.52	219.98	259.0
Moxifloxacin	122.13	113.16	101.8	48.42	46.45	40.4	60.04	60.17	60.6	340.76	322.44	285.0
4-Aminosalicyclic acid	40.86	43.20	39.3	16.18	16.67	15.6	58.56	58.41	83.4	117.86	119.49	102.7
Pyrazinamide	34.92	41.04	31.9	13.82	14.61	12.6	58.45	60.16	60.7	101.59	109.90	87.7
Rifampin	204.17	158.04	213.1	80.96	73.57	84.5	61.54	61.15	48.0	565.78	503.21	611.7
Terizidone	78.78	74.88	76.1	31.22	30.01	30.2	59.25	60.02	62.5	221.88	202.46	198.9

Table 10
Experimental and actual data for prediction of NM2 and physical properties of antituberculosis drugs.

Medicine	Pred. (LR1)	Pred. (SVR1)	Bp	Pred. (LR2)	Pred. (SVR2)	Mp	Pred. (LR3)	Pred. (SVR3)	Fp	LR4	SVR4	Ev
Amikacin	717.63	672.18	981.8	199.96	183.01	203.5	394.96	359.20	547.6	113.79	104.09	162.2
Bedaquiline	728.87	681.18	702.7	201.02	193.89	176	401.38	364.26	378.8	115.13	106.55	108
Clofazimine	655.32	631.91	566.9	194.06	181.05	210	359.41	331.35	296.7	106.37	88.03	85.1
Delamanid	695.16	668.31	653.7	197.83	194.94	193	382.14	350.50	349.1	111.11	95.36	96.3
Ethambutol	305.29	314.04	345.3	160.94	165.38	89	159.70	180.45	113.7	64.69	66.68	68.3
Ethionamide	317.55	353.91	247.9	162.10	164.88	163	166.69	184.57	103.7	66.14	67.58	46.5
Imipenem	570.20	556.83	530.2	186.01	189.39	180	310.84	291.67	274.5	96.23	90.99	92.7
Isoniazid	287.59	333.48	251.97	159.26	175.74	172	149.60	171.79	251	62.58	65.29	92.1
Levofloxacin	587.22	561.88	571.5	187.62	180.05	224	320.56	298.76	299.4	98.26	90.83	90.1
Linezolid	501.08	489.54	585.5	179.47	179.59	177	271.41	259.14	307.9	88.00	97.59	87.5
Moxifloxacin	704.69	677.17	636.0	198.74	190.90	270	387.58	355.16	338.7	112.25	99.76	98.8
4-Aminosalicyclic acid	316.53	327.66	380.8	162.00	164.68	145	166.11	183.92	184.1	66.02	67.50	66.3
Pyrazinamide	292.69	336.87	173.3	159.75	169.40	190	152.51	176.76	119.1	63.18	71.77	54.1
Rifampin	1000.59	822.91	937.4	226.74	179.59	183	556.41	435.37	561.3	147.48	90.66	153.5
Terizidone	453.75	451.79	569.2	174.99	180.36	175	244.40	238.45	298.1	82.36	79.63	92.1

Table 11
(Cont'd) experimental and actual data for prediction of NM2 and physical properties of antituberculosis drugs.

Medicine	Pred. (LR5)	Pred. (SVR5)	MR	Pred. (LR6)	Pred. (SVR6)	P	Pred. (LR7)	Pred. (SVR7)	ST	Pred. (LR8)	Pred. (SVR8)	Mv
Amikacin	134.41	134.99	134.9	53.29	53.17	53.5	60.55	55.23	103.3	373.81	385.78	363.9
Bedaquiline	137.01	137.96	156.2	54.32	54.41	61.9	60.62	56.80	52.6	380.89	373.18	420.1
Clofazimine	120.01	116.76	136.2	47.58	46.35	54.0	60.19	57.49	47.1	334.56	314.33	366.1
Delamanid	129.22	129.40	127.7	51.23	51.14	50.6	60.42	57.13	50.0	359.66	45.84	368.0
Ethambutol	39.15	39.47	58.6	15.50	15.59	23.2	58.14	57.48	38.1	114.05	117.90	207.0
Ethionamide	41.98	41.38	49	16.63	16.36	19.4	58.21	57.48	39.8	121.78	123.34	142.0
Imipenem	100.35	95.48	72.7	39.78	38.27	28.8	59.69	55.23	71.0	280.94	275.46	183.9
Isoniazid	35.06	45.05	36.9	13.88	17.72	14.6	58.04	56.17	57.8	102.90	120.92	110.2
Levofloxacin	104.28	100.22	91.1	41.34	39.94	36.1	59.79	55.23	70.3	291.66	287.52	244.0
Linezolid	84.38	77.67	83	33.44	30.58	32.9	59.29	57.44	47.7	237.39	209.85	259.0
Moxifloxacin	131.42	131.79	101.8	52.10	52.18	40.4	60.48	55.82	60.6	365.66	375.56	285.0
4-Aminosalicyclic acid	41.75	48.76	39.3	16.53	19.24	15.6	58.21	55.23	83.4	121.13	128.38	102.7
Pyrazinamide	36.24	45.66	31.9	14.35	17.97	12.6	58.07	55.81	60.7	106.12	121.63	87.7
Rifampin	199.78	185.24	213.1	79.22	76.61	84.5	62.20	57.40	48.0	552.07	520.10	611.7
Terizidone	73.45	66.98	76.1	29.11	26.38	30.2	59.01	55.59	62.5	207.58	193.90	198.9

Table 12
Experimental and actual data for prediction of NR and physical properties of antituberculosis drugs.

Medicine	Pred. (LR1)	Pred. (SVR1)	Bp	Pred. (LR2)	Pred. (SVR2)	Mp	Pred. (LR3)	Pred. (SVR3)	Fp	LR4	SVR4	Ev
Amikacin	708.60	673.77	981.8	200.84	186.95	203.5	389.62	356.07	547.6	112.78	114.21	162.2
Bedaquiline	688.81	669.05	702.7	198.76	192.94	176	378.35	350.53	378.8	110.42	109.65	108
Clofazimine	636.95	579.55	566.9	193.31	188.08	210	348.82	336.07	296.7	104.22	102.29	85.1
Delamanid	683.35	686.25	653.7	198.19	189.13	193	375.24	349.17	349.1	109.76	96.80	96.3
Ethambutol	392.65	487.32	345.3	167.65	177.90	89	209.71	266.61	113.7	75.03	98.63	68.3
Ethionamide	329.19	276.91	247.9	160.98	173.48	163	173.58	248.81	103.7	67.44	46.28	46.5
Imipenem	411.76	393.17	530.2	169.65	169.42	180	220.59	271.84	274.5	77.31	85.48	92.7
Isoniazid	337.37	284.29	251.97	161.84	170.15	172	178.24	250.40	251	68.42	70.44	92.1
Levofloxacin	508.66	585.40	571.5	179.83	177.10	224	275.77	299.53	299.4	88.89	87.60	90.1
Linezolid	508.66	571.40	585.5	179.83	190.14	177	275.77	299.36	307.9	88.89	90.20	87.5
Moxifloxacin	860.10	660.46	636.0	216.76	183.00	270	475.88	405.91	338.7	130.88	100.86	98.8
4-Aminosalicyclic acid	336.01	256.10	380.8	161.70	172.26	145	177.46	250.72	184.1	68.26	84.34	66.3
Pyrazinamide	302.57	329.77	173.3	158.18	174.36	190	158.42	241.41	119.1	64.26	83.15	54.1
Rifampin	946.76	558.79	937.4	225.86	189.14	183	525.23	412.14	561.3	141.24	94.40	153.5
Terizidone	482.73	603.97	569.2	177.11	187.73	175	261.00	291.97	298.1	85.79	98.55	92.1

Table 13
(Cont'd) experimental and actual data for prediction of NR and physical properties of antituberculosis drugs.

Medicine	Pred. (LR5)	Pred. (SVR5)	MR	Pred. (LR6)	Pred. (SVR6)	P	Pred. (LR7)	Pred. (SVR7)	ST	Pred. (LR8)	Pred. (SVR8)	Mv
Amikacin	132.18	133.77	134.9	52.41	53.09	53.5	59.63	52.16	103.3	369.72	384.67	363.9
Bedaquiline	127.62	129.09	156.2	50.60	51.22	61.9	59.61	53.14	52.6	357.06	352.39	420.1
Clofazimine	115.69	116.74	136.2	45.86	46.29	54.0	59.58	54.13	47.1	323.89	321.52	366.1
Delamanid	126.37	128.94	127.7	50.10	51.17	50.6	59.61	53.22	50.0	353.57	349.16	368.0
Ethambutol	59.46	54.37	58.6	23.56	21.66	23.2	59.44	58.85	38.1	167.66	172.07	207.0
Ethionamide	44.86	38.58	49	17.76	15.34	19.4	59.40	60.08	39.8	127.07	133.64	142.0
Imipenem	63.86	59.17	72.7	25.30	23.57	28.8	59.45	56.77	71.0	179.88	189.16	183.9
Isoniazid	46.74	45.68	36.9	18.51	18.08	14.6	59.40	59.92	57.8	132.31	146.47	110.2
Levofloxacin	86.16	83.75	91.1	34.15	33.28	36.1	59.51	55.28	70.3	241.85	247.51	244.0
Linezolid	86.16	86.65	83	34.15	34.35	32.9	59.51	56.62	47.7	241.85	243.84	259.0
Moxifloxacin	167.04	171.27	101.8	66.24	68.16	40.4	59.72	49.56	60.6	466.60	483.76	285.0
4-Aminosalicyclic acid	46.43	45.36	39.3	18.39	17.95	15.6	59.40	57.92	83.4	131.43	145.71	102.7
Pyrazinamide	38.73	37.66	31.9	15.33	14.83	12.6	59.38	58.42	60.7	110.05	127.28	87.7
Rifampin	186.99	184.70	213.1	74.15	74.28	84.5	59.77	60.21	48.0	522.02	484.95	611.7
Terizidone	80.19	80.37	76.1	31.78	31.88	30.2	59.49	55.68	62.5	225.26	230.88	198.9

Table 14
Experimental and actual data for prediction of NRR and physical properties of antituberculosis drugs.

Medicine	Pred. (LR1)	Pred. (SVR1)	Bp	Pred. (LR2)	Pred. (SVR2)	Mp	Pred. (LR3)	Pred. (SVR3)	Fp	LR4	SVR4	Ev
Amikacin	735.16	563.72	981.8	199.95	192.25	203.5	405.09	381.21	547.6	115.88	108.27	162.2
Bedaquiline	728.96	591.96	702.7	199.41	194.94	176	401.55	378.94	378.8	115.14	107.78	108
Clofazimine	669.14	591.70	566.9	194.27	228.98	210	367.38	349.28	296.7	108.02	101.19	85.1
Delamanid	731.62	646.98	653.7	199.64	195.37	193	403.07	380.53	349.1	115.46	108.41	96.3
Ethambutol	316.64	363.53	345.3	163.97	162.74	89	166.03	187.65	113.7	66.03	66.62	68.3
Ethionamide	315.29	345.87	247.9	163.86	160.98	163	165.26	187.46	103.7	65.87	68.32	46.5
Imipenem	506.14	595.23	530.2	180.26	183.05	180	274.27	265.46	274.5	88.6	83.17	92.7
Isoniazid	289.24	254.87	251.97	161.61	170.24	172	150.38	174.19	251	62.77	64.85	92.1
Levofloxacin	571.71	591.25	571.5	185.90	193.19	224	311.72	298.77	299.4	96.41	91.03	90.1
Linezolid	514.50	589.91	585.5	180.97	188.69	177	279.05	269.55	307.9	89.6	84.0	87.5
Moxifloxacin	662.11	584.78	636.0	193.67	211.83	270	363.36	345.73	338.7	107.18	100.42	98.8
4-Aminosalicyclic acid	313.40	425.77	380.8	163.69	163.63	145	164.18	187.19	184.1	65.64	68.21	66.3
Pyrazinamide	288.77	266.68	173.3	161.58	170.29	190	150.11	185.00	119.1	62.71	66.91	54.1
Rifampin	1012.58	555.95	937.4	223.79	187.58	183	563.55	386.63	561.3	148.93	106.32	153.5
Terizidone	478.90	591.47	569.2	177.92	170.13	175	258.71	252.51	298.1	85.36	80.54	92.1

Table 15
(Cont'd) experimental and actual data for prediction of NRR and physical properties of antituberculosis drugs.

Medicine	Pred. (LR5)	Pred. (SVR5)	MR	Pred. (LR6)	Pred. (SVR6)	P	Pred. (LR7)	Pred. (SVR7)	ST	Pred. (LR8)	Pred. (SVR8)	Mv
Amikacin	138.80	130.15	134.9	55.03	54.18	53.5	60.27	57.33	103.3	386.49	370.48	363.9
Bedaquiline	137.36	128.86	156.2	54.46	52.80	61.9	60.25	58.01	52.6	382.54	359.99	420.1
Clofazimine	123.43	116.19	136.2	48.93	47.02	54.0	60.02	62.73	47.1	344.34	320.08	366.1
Delamanid	137.98	133.97	127.7	54.70	53.80	50.6	60.26	63.33	50.0	384.23	361.72	368.0
Ethambutol	41.38	40.08	58.6	16.39	16.02	23.2	58.66	36.97	38.1	119.29	119.64	207.0
Ethionamide	41.06	39.80	49	16.26	15.91	19.4	58.65	55.46	39.8	118.43	119.15	142.0
Imipenem	85.49	82.13	72.7	33.88	32.26	28.8	59.39	60.60	71.0	240.27	215.62	183.9
Isoniazid	34.99	34.37	36.9	13.86	13.80	14.6	58.55	60.83	57.8	101.80	127.76	110.2
Levofloxacin	100.75	96.68	91.1	39.94	38.15	36.1	59.64	60.67	70.3	282.14	258.26	244.0
Linezolid	87.43	83.96	83	34.66	32.95	32.9	59.42	62.67	47.7	245.61	216.93	259.0
Moxifloxacin	121.79	117.78	101.8	48.29	46.63	40.4	59.99	61.51	60.6	339.85	320.44	285.0
4-Aminosalicyclic acid	40.62	41.76	39.3	16.09	16.50	15.6	58.64	52.80	83.4	117.22	130.66	102.7
Pyrazinamide	34.89	36.91	31.9	13.81	14.67	12.6	58.55	58.05	60.7	101.49	127.72	87.7
Rifampin	203.38	182.27	213.1	80.65	72.79	84.5	61.34	62.65	48.0	563.61	466.27	611.7
Terizidone	79.15	75.48	76.1	31.37	29.68	30.2	59.28	61.36	62.5	222.88	195.30	198.9

Table 16
Experimental and actual data for prediction of NHP and physical properties of antituberculosis drugs.

Medicine	Pred. (LR1)	Pred. (SVR1)	Bp	Pred. (LR2)	Pred. (SVR2)	Mp	Pred. (LR3)	Pred. (SVR3)	Fp	LR4	SVR4	Ev
Amikacin	735.68	704.36	981.8	201.55	173.92	203.5	405.39	390.63	547.6	116.14	98.44	162.2
Bedaquiline	725.82	777.73	702.7	200.62	197.53	176	399.75	394.37	378.8	114.95	101.03	108
Clofazimine	648.25	594.03	566.9	193.33	180.39	210	355.45	312.29	296.7	105.64	92.56	85.1
Delamanid	687.70	605.64	653.7	197.04	185.70	193	377.98	334.02	349.1	110.37	91.28	96.3
Ethambutol	305.74	277.48	345.3	161.13	166.62	89	159.80	172.67	113.7	64.49	73.97	68.3
Ethionamide	317.01	379.11	247.9	162.18	163.98	163	166.24	183.57	103.7	65.85	72.35	46.5
Imipenem	578.06	573.10	530.2	186.73	191.74	180	315.35	300.16	274.5	97.20	90.27	92.7
Isoniazid	288.09	358.63	251.97	159.47	181.23	172	149.72	113.97	299.4	62.37	76.03	92.1
Levofloxacin	586.59	535.22	571.5	187.53	180.19	224	320.23	283.25	307.9	98.23	92.43	90.1
Linezolid	489.22	580.28	585.5	178.38	180.62	177	264.60	302.46	338.7	86.53	91.55	87.5
Moxifloxacin	707.01	636.02	636.0	198.86	182.63	270	389.01	357.86	184.1	112.69	101.22	98.8
4-Aminosalicyclic acid	317.42	380.64	380.8	162.22	164.11	145	166.47	147.98	119.1	65.90	72.49	66.3
Pyrazinamide	292.31	322.69	173.3	159.86	169.45	190	152.13	162.03	561.3	62.88	85.76	54.1
Rifampin	1004.02	543.86	937.4	226.78	180.46	183	558.67	429.06	298.1	148.37	89.19	153.5
Terizidone	451.26	584.55	569.2	174.81	181.25	175	242.92	269.61		81.97	90.23	92.1

Table 17
(Cont'd) experimental and actual data for prediction of NHP and physical properties of antituberculosis drugs.

Medicine	Pred. (LR5)	Pred. (SVR5)	MR	Pred. (LR6)	Pred. (SVR6)	P	Pred. (LR7)	Pred. (SVR7)	ST	Pred. (LR8)	Pred. (SVR8)	Mv
Amikacin	138.19	138.47	134.9	54.79	60.72	53.5	60.996	55.23	103.3	383.98	314.52	363.9
Bedaquiline	135.93	132.80	156.2	53.89	52.00	61.9	60.92	56.80	52.6	377.83	296.84	420.1
Clofazimine	118.17	114.58	136.2	46.85	41.14	54.0	60.33	57.49	47.1	329.45	276.11	366.1
Delamanid	127.20	124.00	127.7	50.43	46.04	50.6	60.63	57.13	50.0	354.05	276.00	368.0
Ethambutol	39.73	39.00	58.6	15.73	16.11	23.2	57.73	57.49	38.1	115.81	258.76	207.0
Ethionamide	42.31	40.47	49	16.75	16.95	19.4	57.82	57.49	39.8	122.84	102.43	142.0
Imipenem	102.09	104.91	72.7	40.47	39.67	28.8	59.80	55.23	71.0	285.66	274.50	183.9
Isoniazid	35.68	47.13	36.9	14.13	16.89	14.6	57.60	56.18	57.8	104.80	135.38	110.2
Levofloxacin	104.05	106.99	91.1	41.25	40.44	36.1	59.86	55.23	70.3	290.99	249.91	244.0
Linezolid	81.75	76.82	83	32.40	31.75	32.9	59.12	57.44	47.7	230.25	286.97	259.0
Moxifloxacin	131.63	131.61	101.8	52.19	54.13	40.4	60.78	55.82	60.6	366.09	285.52	285.0
4-Aminosalicyclic acid	42.40	49.15	39.3	16.79	19.35	15.6	57.82	55.23	83.4	123.10	143.36	102.7
Pyrazinamide	36.65	47.25	31.9	14.51	17.06	12.6	57.63	55.81	60.7	107.43	146.73	87.7
Rifampin	199.65	111.17	213.1	79.17	40.60	84.5	63.03	57.40	48.0	551.36	259.51	611.7
Terizidone	73.06	71.04	76.1	28.95	31.22	30.2	58.84	55.59	62.5	206.58	293.06	198.9

Table 18
Experimental and actual data for prediction of NHM and physical properties of antituberculosis drugs.

Medicine	Pred. (LR1)	Pred. (SVR1)	Bp	Pred. (LR2)	Pred. (SVR2)	Mp	Pred. (LR3)	Pred. (SVR3)	Fp	LR4	SVR4	Ev
Amikacin	754.29	702.01	981.8	195.67	192.91	203.5	416.79	352.60	547.6	118.80	110.46	162.2
Bedaquiline	745.40	702.44	702.7	195.16	193.45	176	411.68	350.52	378.8	117.71	117.37	108
Clofazimine	684.81	493.77	566.9	191.64	192.13	210	376.85	338.66	296.7	110.31	109.57	85.1
Delamanid	738.94	670.21	653.7	194.78	193.55	193	407.96	354.43	349.1	116.92	116.52	96.3
Ethambutol	391.51	499.78	345.3	174.62	176.60	89	208.24	269.61	113.7	74.50	73.71	68.3
Ethionamide	320.41	235.41	247.9	170.49	171.48	163	167.37	253.48	103.7	65.81	66.17	46.5
Imipenem	412.52	406.38	530.2	175.83	170.73	180	220.32	271.65	274.5	77.06	74.89	92.7
Isoniazid	330.10	276.58	251.97	171.05	163.90	172	172.94	255.67	251	67.00	65.54	92.1
Levofloxacin	528.87	577.78	571.5	182.59	184.64	224	287.20	301.06	299.4	91.27	87.25	90.1
Linezolid	532.10	584.83	585.5	182.78	186.67	177	289.06	300.07	307.9	91.66	90.39	87.5
Moxifloxacin	544.22	606.46	636.0	183.48	185.60	270	296.03	302.95	338.7	93.14	88.90	98.8
4-Aminosalicyclic acid	328.49	251.46	380.8	170.96	171.99	145	172.02	255.30	184.1	66.80	65.82	66.3
Pyrazinamide	290.51	349.09	173.3	168.75	160.62	190	150.19	246.75	119.1	62.16	64.41	54.1
Rifampin	1029.81	543.09	937.4	211.67	194.81	183	575.17	405.23	561.3	152.44	132.34	153.5
Terizidone	502.20	522.67	569.2	181.04	184.89	175	271.88	292.96		88.01	84.39	92.1

Table 19
(Cont'd) experimental and actual data for prediction of NHM and physical properties of antituberculosis drugs.

Medicine	Pred. (LR5)	Pred. (SVR5)	MR	Pred. (LR6)	Pred. (SVR6)	P	Pred. (LR7)	Pred. (SVR7)	ST	Pred. (LR8)	Pred. (SVR8)	Mv
Amikacin	144.71	148.60	134.9	57.37	58.36	53.5	59.38	52.55	103.3	404.51	387.97	363.9
Bedaquiline	142.58	142.86	156.2	56.53	56.84	61.9	59.38	53.02	52.6	398.59	371.52	420.1
Clofazimine	128.06	128.33	136.2	50.77	50.83	54.0	59.43	54.07	47.1	358.25	337.35	366.1
Delamanid	141.03	144.76	127.7	55.91	56.86	50.6	59.39	53.13	50.0	394.29	376.78	368.0
Ethambutol	57.77	56.42	58.6	22.89	22.44	23.2	59.63	59.07	38.1	162.96	172.28	207.0
Ethionamide	40.73	39.11	49	16.13	15.43	19.4	59.68	60.28	39.8	115.62	133.77	142.0
Imipenem	62.80	61.47	72.7	24.89	24.58	28.8	59.62	57.59	71.0	176.95	190.08	183.9
Isoniazid	43.05	44.58	36.9	17.05	17.28	14.6	59.68	60.11	57.8	122.07	146.85	110.2
Levofloxacin	90.69	89.35	91.1	35.95	35.75	36.1	59.54	56.45	70.3	254.42	253.20	244.0
Linezolid	91.46	92.02	83	36.25	36.52	32.9	59.53	56.69	47.7	256.57	250.59	259.0
Moxifloxacin	94.36	93.09	101.8	37.40	37.21	40.4	59.53	56.19	60.6	264.64	257.43	285.0
4-Aminosalicyclic acid	42.66	44.23	39.3	16.90	17.15	15.6	59.68	58.56	83.4	120.99	146.02	102.7
Pyrazinamide	33.56	36.12	31.9	13.29	13.65	12.6	59.71	58.92	60.7	95.71	126.85	87.7
Rifampin	210.74	183.65	213.1	83.56	81.73	84.5	59.18	47.73	60.7	587.96	488.82	611.7
Terizidone	84.30	84.48	76.1	33.41	33.57	30.2	59.56	56.76	62.5	236.66	238.62	198.9

Table 20
Performance measures for LR and SVR of NGA.

Physical Properties	LR RMSE	C	γ	SVR RMSE
Bp	93.88	1000	0.0001	86.4
Mp	34.49	400	0.02	17.09
Fp	59.49	500	0.0001	58.36
Ev	17.75	150	0.0001	13.63
MR	8.38	1000	0.0001	6.57
P	3.16	500	0.0001	2.54
ST	16.65	10	0.01	11.85
Mv	31.16	1000	0.0001	30.44

Table 21
Performance measures for LR and SVR of NABC.

Physical Properties	LR RMSE	C	γ	SVR RMSE
Bp	91.36	1000	0.005	87.55
Mp	35.42	500	0.2	16.90
Fp	60.28	800	0.005	59.66
Ev	17.24	700	0.0001	14.48
MR	8.30	1000	0.0001	7.25
P	3.29	500	0.0001	2.83
ST	16.66	300	0.0001	12.19
Mv	25.43	1000	0.0001	32.50

Table 22
Performance measures for LR and SVR of NM1.

Physical Properties	LR RMSE	C	γ	SVR RMSE
Bp	89.66	400	0.000001	80.08
Mp	33.39	50	0.0001	19.48
Fp	57.11	500	0.000001	51.25
Ev	17.35	280	0.000001	17.27
MR	11.06	1000	0.00001	11.66
P	4.38	800	0.0000001	4.02
ST	16.63	1000	10	12.77
Mv	38.65	1000	0.000001	35.07

Our aim is to obtain a prediction using SVR that will perform better than the classical LR model and also establish a relationship between the independent variable and dependent variable. Our dataset is very small, it consists of 120 data points of independent and dependent variables which is divided into eight columns (15 data points per column) (see Table 1 and Table 3 respectively). Given the nature of the data and the desire for improved predictions with reduced error, we performed SVR modelling with LOOCV using Algorithm 1. We chose the RBF kernel due to its ability to model high-dimensional feature spaces, where data points may not be linearly separable. It can map data into a higher-dimensional space, making it easier to find a separating hyperplane. The γ parameter is chosen for our RBF kernel trick, we chose γ values within the range $\gamma = [0.0000001, 10]$, we chose the smallest γ value possible so that the model can consider a broader range of data points when making predictions instead of focusing on the data points that are very close to the support vectors as is the case of large γ parameter which can lead to a more complex and possibly overfit model. Smaller γ parameter leads to a smoother and more generalized model and is less sensitive to individual data points and is more likely to generalize well. We also chose our C parameter within the range of $C = [1, 1000]$, we chose the upper limit of 1000 so that our SVR model can prioritize minimizing the training error. In summary, the choice of the optimal γ value and C value are determined through hyperparameter tuning technique called the grid search method, this is based on LOOCV of SVR. The grid search method carries out hyperparameter tuning by searching through the range of C and γ defined and then selects the best values that predicts our model with the smallest error (RMSE) possible.

We proceed to analyze the performance measurements of our models across multiple tables. In Table 20, which represents a QSPR model of the NGA and physical properties of antituberculosis drugs, the SVR model exhibited lower RMSE values for all eight physical properties considered, indicating its superior performance over LR model. Similarly, in Table 21, SVR model achieved lower RMSE values for seven physical properties, except for Mv, where LR outperformed SVR. This suggests that SVR outperformed LR in the QSPR model for the NABC index and physical properties of antituberculosis drugs.

Moving on to Table 22, SVR outperformed LR in seven out of eight physical properties in the QSPR model between the NM1 index and physical properties, with LR performing better only in the case of MR.

In Table 23, SVR consistently outperformed LR throughout the QSPR model for the NM2 index and physical properties of antituberculosis drugs, as indicated by the lower RMSE values obtained by SVR model.

Algorithm 1 Radial kernel LOOCV for QSPR model of antituberculosis.

Require:
Dataset with features x and target variable y
Radial Kernel parameters
Ensure:
QSPR model for predicting physical properties
procedure RADIAL KERNEL LOOCV($x, y,$ kernel parameters)
  for each data point i in x **do**
    Leave-One-Out:
      Create training set x_{train} by excluding data point i
      Create test set x_{test} with only data point i
    Train the SVR model:
      Use radial kernel with parameters (C and γ)
      Train SVR model on x_{train} and y_{train}
    Predict the target variable:
      Predict y_{pred} for data point i using the trained model
    Evaluate the model:
      Calculate performance metric (RMSE) for y_{pred} and y_i
  end for
  Aggregate performance metrics:
    Calculate the overall performance of the QSPR model
  Optimize kernel parameters:
    Adjust kernel parameters based on LOOCV results
  Train final QSPR model:
    Use optimized parameters and the entire dataset
  Return the final QSPR model predictions
end procedure

Table 23
Performance measures for LR and SVR of NM2.

Physical Properties	LR RMSE	C	γ	SVR RMSE
Bp	95.61	800	0.0000001	83.43
Mp	32.47	10	0.0001	22.35
Fp	60.57	400	0.0000001	52.82
Ev	17.91	50	0.00001	14.71
MR	14.35	1000	0.0000001	13.45
P	5.69	1000	0.0000001	5.19
ST	16.61	10	10	13.55
Mv	48.15	1000	0.0000001	46.14

Table 24
Performance measures for LR and SVR of NR.

Physical Properties	LR RMSE	C	γ	SVR RMSE
Bp	114.64	300	1	98.28
Mp	31.78	10	1	25.33
Fp	70.87	1000	0.0008	65.38
Ev	19.33	1000	10	16.44
MR	20.86	1000	0.001	14.06
P	8.26	900	0.0004	5.48
ST	16.66	500	0.004	13.41
Mv	58.66	1000	0.002	46.36

Table 24 demonstrates the superiority of SVR over LR in the QSPR model for the NR index and physical properties of antituberculosis drugs. SVR obtained lower RMSE values for all physical properties considered.

In Table 25, SVR outperformed LR in six of the physical properties in the QSPR model of NRR index, but LR achieved lower RMSE values for phsycal properties of Bp and Mv.

For the QSPR model of the NHP index, Table 26 indicates that SVR outperformed LR in predicting five physical properties, while LR performed better in predicting MR, P, and Mv.

Lastly, in Table 27, SVR performed better in predicting physical properties in the QSPR model for the NHM index, while LR exhibited superior performance in predicting MR, P, and Mv.

The impact of lower RMSE suggests that the model's predictions are more accurate and the model's predicted values are on average closer to the actual values of the physical properties, indicating that the model is better at estimating the relationship between the neighbourhood degree-based TI and the corresponding physical properties of antituberculosis drugs. From Tables 20 - 27, there is a total of 64 regression metric of physical properties recorded for both the LR and SVR which is divided across eight neighbourhood degree-based TI. The SVR obtained the lower RMSE values in 54 of the regression metric of physical properties

Table 25
Performance measures for LR and SVR of NRR.

Physical Properties	LR RMSE	C	γ	SVR RMSE
Bp	90.47	350	1	90.79
Mp	33.72	50	0.0005	18.70
Fp	57.67	350	0.00001	55.29
Ev	17.52	100	0.00001	14.81
MR	10.93	1000	0.000001	10.63
P	4.33	1000	0.000001	3.89
ST	16.64	50	1	12.34
Mv	38.37	300	0.00001	39.15

Table 26
Performance measures for LR and SVR of NHP.

Physical Properties	LR RMSE	C	γ	SVR RMSE
Bp	93.05	270	0.00001	91.74
Mp	32.48	10	0.00001	24.72
Fp	58.99	1000	0.000001	52.35
Ev	17.41	10	0.00001	16.40
MR	14.82	50	0.0001	20.46
P	5.87	150	0.0001	8.64
ST	16.58	10	10	13.55
Mv	49.61	270	0.0001	76.15

Table 27
Performance measures for LR and SVR of NHM.

Physical Properties	LR RMSE	C	γ	SVR RMSE
Bp	98.22	1000	2	97.84
Mp	35.95	60	0.02	24.76
Fp	60.23	1000	0.0005	65.94
Ev	17.24	1000	0.001	15.37
MR	7.94	1000	0.002	9.96
P	3.14	500	0.005	3.12
ST	16.66	1000	0.0004	11.89
Mv	23.95	900	0.002	32.41

recorded across the eight neighbourhood degree-based TI while the LR obtained lower RMSE value in only 10 of the regression metric of physical properties across eight neighbourhood degree-based TI. From this, we confirm that the SVR is a better prediction model in QSPR analysis of the physical properties of antituberculosis drugs.

Below are the equations for the LR model. The equations were obtained using (12). The coefficient of each neighbourhood degree-based TI and the constant or intercept term is used to formulate the model, the intercept is the first term in each equation, it represents the predicted value when all input variables are zero. A positive or negative intercept indicates a shift in the predicted data.

$$Bp = 135.26 + 26.83[NABC]$$
$$Mp = 154.41 + 1.06[NGA]$$
$$Fp = 95.17 + 0.64[NM1]$$
$$Ev = 54.79 + 0.04[NM2]$$
$$MR = 7.79 + 15.71[NR]$$
$$P = 4.98 + 0.21[NRR]$$
$$ST = 57.09 + 0.001[NHP]$$
$$Mv = -8.66 + 53.8[NHM].$$

4.2. Performance measure for neighbourhood degree-based TI

In this subsection, we present the comparative model plots for all the neighbourhood degree-based TI. The plot compares the RMSE values between different neighbourhood degree-based TIs of the LR and SVR models for the physical properties of antituberculosis drugs. By comparing the LR and SVR lines, one can observe the differences in their RMSE values across the different

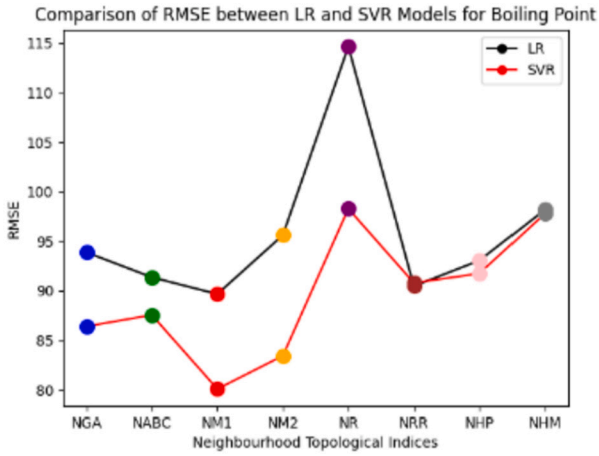

Fig. 17. RMSE of SVR and LR models for Bp vs TIs.

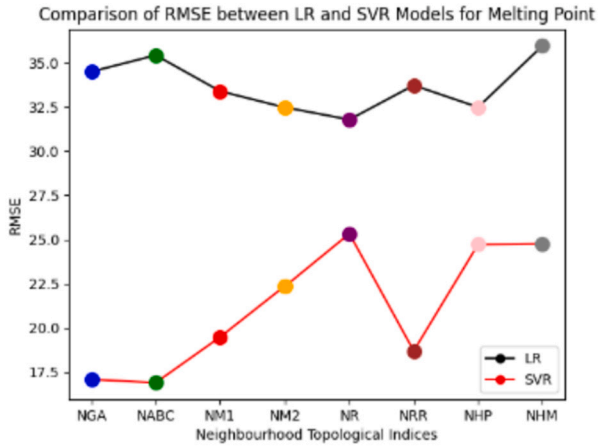

Fig. 18. RMSE of SVR and LR models for Mp vs TIs.

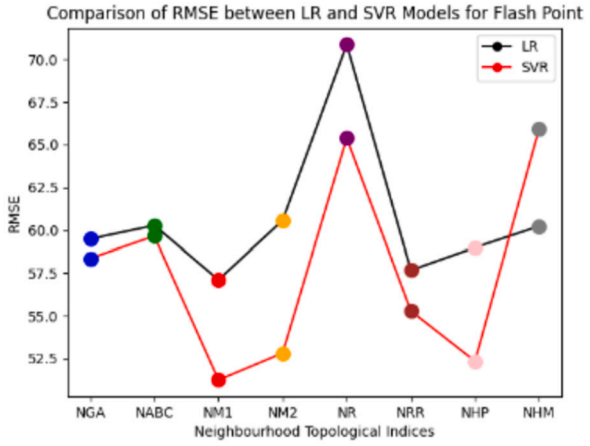

Fig. 19. RMSE of SVR and LR models for Fp vs TIs.

neighbourhood degree-based TIs. If the SVR line consistently stays below the LR line, it indicates that the SVR model generally outperforms the LR model in terms of accuracy and predictive power for the physical property. Conversely, if the LR line consistently stays below the SVR line, it suggests that the LR model performed better. The following are plots (Figs. 17 - 24) that show the comparison between the RMSE of SVR and LR models across different neighbourhood TIs.

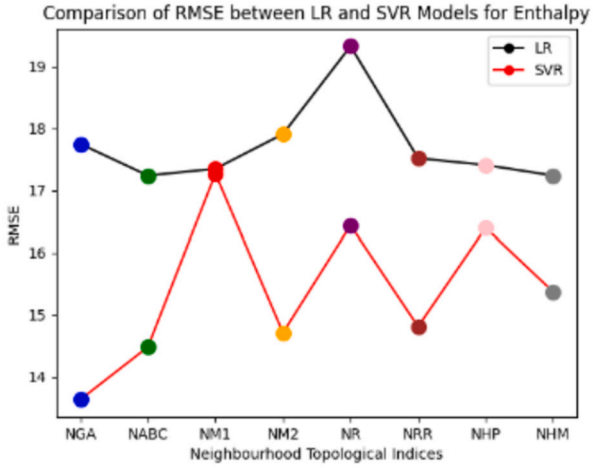

Fig. 20. RMSE of SVR and LR models for Ev vs TIs.

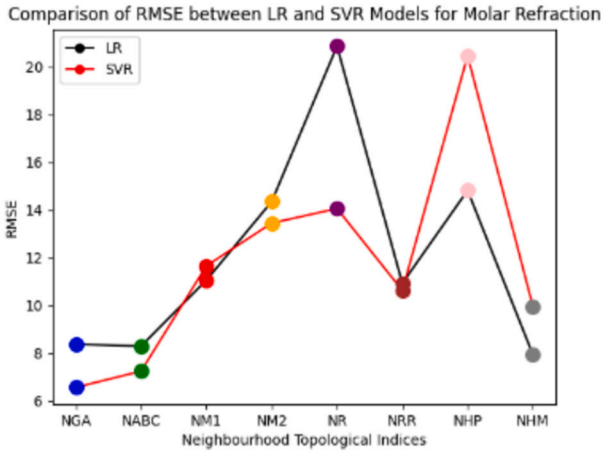

Fig. 21. RMSE of SVR and LR models for MR vs TIs.

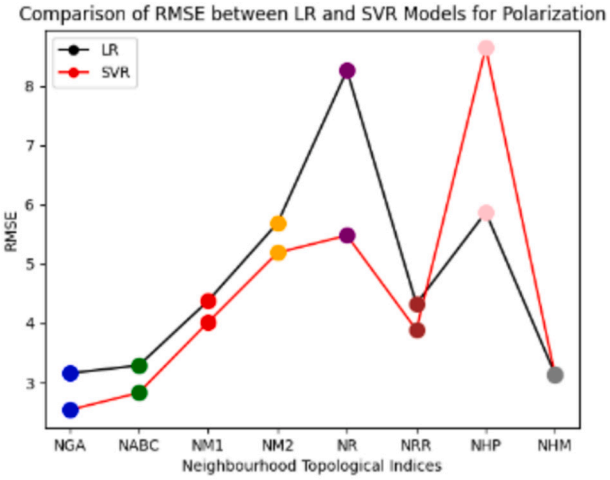

Fig. 22. RMSE of SVR and LR models for P vs TIs.

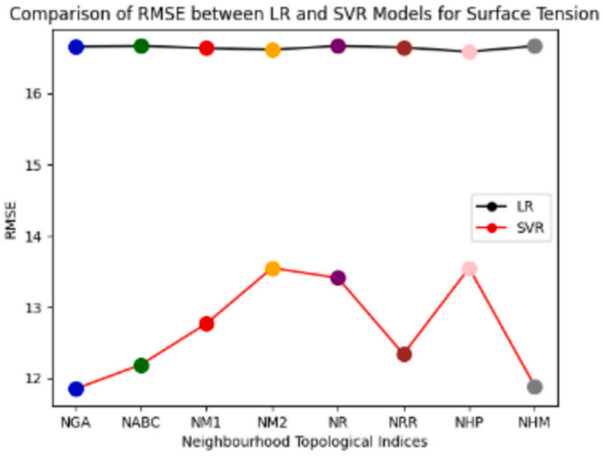

Fig. 23. RMSE of SVR and LR models for ST vs TIs.

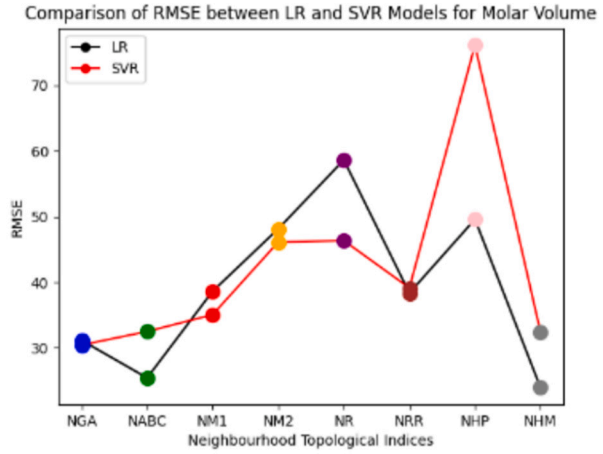

Fig. 24. RMSE of SVR and LR models for Mv vs TIs.

From the plots it is evident that the physical properties where the neighbourhood degree-based TIs of SVR obtained general superiority is in surface tension (Fig. 23) and melting point (Fig. 18), followed by enthalpy of vapourization (Fig. 20) meaning that the neighbourhood degree-based TIs modelled by SVR had a significant difference in RMSE compared to neighbourhood degree-based TIs modelled by LR. This is followed by boiling point (Fig. 17), flash point (Fig. 19), molar refraction (Fig. 21), polarization (Fig. 22) and molar volume (Fig. 24). From the previous literature (see [3]), the melting point and surface tension did not exhibit any correlation with degree-based TIs in the QSPR analysis. However, the use of a combined approach of neighbourhood degree-based TIs and machine learning models has made it possible to achieve improvement in this regard, this is shown in the lower RMSE values recorded for all the neighbourhood degree-based TIs in the SVR model.

5. Conclusion

In this manuscript, we investigated the QSPR analysis of eight physical properties of fifteen antituberculosis drugs using the neighbourhood degree-based TI and SVR model. The findings in this study have provided valuable insights into the importance of neighbourhood degree-based TI in QSPR modelling of drugs and the effectiveness of SVR as a superior predictive model compared to LR model. Through extensive data analysis and experimentation, it has been demonstrated that SVR outperformed LR in predicting the physical properties of antituberculosis drugs. From Tables 20 to 27, the SVR obtained the lower RMSE values in 54 of the regression metric of physical properties recorded across the eight neighbourhood degree-based TI while the LR obtained lower RMSE value in only 10 of the regression metric of physical properties across eight neighbourhood degree-based TI. From this, we conclude that the SVR is a better prediction model in QSPR analysis of the physical properties of antituberculosis drugs.

The best models were obtained in the QSPR analysis of the following neighbourhood degree-based TI; NGA, NM2 and NR, these indices obtained lower RMSE values for SVR throughout their respective model implementations. This is followed by NABC and NM1, where SVR obtained lower RMSE values in seven physical properties. The NRR, NHP and NHM also performed well as the

SVR performed optimally well in 6 out of 8 physical properties of NRR, they also performed optimally well in 5 out of 8 physical properties of the NHP and NHM TIs.

Furthermore, the melting point and surface tension are the physical properties that exhibited substantial differences between the SVR and LR models, with a notable variation in their RMSE values. The enthalpy of vaporization also demonstrated significant distinctions between the two models. Additionally, among all the QSPR analyses conducted using neighbourhood degree-based topological indices, polarization emerged as the physical property that achieved the lowest RMSE values for both the LR and SVR models. Following polarization, molar refraction, surface tension, and enthalpy also demonstrated relatively low RMSE values in the analyses.

Based on the outcomes of this research, it is recommended that researchers in the field of chemical graph theory incorporate neighbourhood degree-based TI and SVR in their QSPR modelling process. Utilizing these advanced techniques can lead to more precise predictions of drug properties, thereby accelerating the predictive ability of drugs and other chemical compounds. The insights gained from this study contribute further to the ongoing research on the designs and construction of efficient TIs and their applications in QSPR modelling of drugs. Finally, we pose some open problems for future research:

(i) Can we investigate the integration of neighbourhood degree-based TI with a more efficient classification model to assess the similarity of chemical compounds found in drugs and classify the toxicity of these compounds?
(ii) Can we explore the possibility of obtaining a larger dataset of drugs or chemical compounds to enhance future QSPR analysis using SVR model, with the goal of improving the accuracy and predictive capabilities of the model.
(iii) Considering the findings of recent studies that suggest the superior efficiency of reverse degree-based TI QSPR models over degree and neighbourhood degree TI (see [6,7]). In order to obtain improved predictive efficiency, can we consider the potential exploration of incorporating modified reverse degree parameters with efficient feature selection techniques of SVR model such as Sequential Backward Search Selection (SBSS) and Exhaustive Search Method (ESM) algorithms?

Funding statement

This research was conducted without external funding. The authors received no specific financial support for the design, data collection, analysis, interpretation, or writing of this research.

CRediT authorship contribution statement

Muhammad Shafii Abubakar: Software, Formal analysis, Data curation. **Kazeem Olalekan Aremu:** Writing – review & editing, Validation, Supervision, Conceptualization. **Maggie Aphane:** Writing – review & editing, Validation, Supervision. **Lateef Babatunde Amusa:** Software.

Declaration of competing interest

The authors declare that they have no known competing financial interests or personal relationships that could have appeared to influence the work reported in this paper.

Data availability

No data associated with this study was deposited into a publicly available library. The data supporting the findings of this study are included in this manuscript.

Acknowledgement

The authors are appreciative of the valuable suggestions provided by the reviewers, which have greatly improved the manuscript.

References

[1] M.S. Abubakar, K.O. Aremu, M. Aphane, Neighborhood versions of geometric–arithmetic and atom bond connectivity indices of some popular graphs and their properties, Axioms 11 (9) (2022) 487, https://doi.org/10.3390/axioms11090487.
[2] N. Ardeshir, C. Sanford, D.J. Hsu, Support vector machines and linear regression coincide with very high-dimensional features, Adv. Neural Inf. Process. Syst. 34 (2021) 4907–4918.
[3] M. Adnan, S.A.U.H. Bokhary, G. Abbas, T. Iqbal, Degree-based topological indices and QSPR analysis of antituberculosis drugs, Hindawi J. Chem. (2022), https://doi.org/10.1155/2022/5748626.
[4] S. Ahmed, S. Nandi, A.K. Saxena, An updated patent review on drugs for the treatment of tuberculosis (2018-present), Expert Opin. Ther. Pat. 32 (3) (2022) 243–260.
[5] A. Anzueto, M.S. Niederman, J. Pearle, M.I. Restrepo, A. Heyder, S.H. Choudhri, Community-Acquired Pneumonia Recovery in the Elderly Study Groupat, Community-acquired pneumonia recovery in the elderly (CAPRIE): efficacy and safety of moxifloxacin therapy versus that of levofloxacin therapy, Clin. Infect. Dis. 42 (1) (2006) 73–81.
[6] M. Arockiaraj, A. Berin Greeni, A.R. Abul Kalaam, Comparative analysis of reverse degree and entropy topological indices for drug molecules in blood cancer treatment through QSPR regression models, polycyclic aromatic compounds, https://doi.org/10.1080/10406638.2023.2271648, 2023.

[7] M. Arockiaraj, A.B. Greeni, A.A. Kalaam, Linear versus cubic regression models for analyzing generalized reverse degree based topological indices of certain latest corona treatment drug molecules, Int. J. Quant. Chem. e27136 (2023).
[8] M. Arockiaraj, J.H. Campenab, A. Berin Greeni, et al., QSPR analysis of distance-based structural indices for drug compounds in tuberculosis treatment, Heliyon 9 (2024) e23981, https://doi.org/10.1016/j.heliyon.2024.e23981.
[9] M. Awad, R. Khanna, Efficient Learning Machines: Theories, Concepts, and Applications for Engineers and System Designers, Springer Nature, 2015, p. 268.
[10] Y. Baştanlar, M. Özuysal, Introduction to machine learning, miRNomics: MicroRNA Biol. Comput. Anal. (2014) 105–128.
[11] B. Bollobás, P. Erdős, Extremal graphs for weight, Ars Comb. 50 (1998) 225.
[12] G. Chartrand, P. Zhang, A First Course in Graph Theory, Courier Corporation, 2013.
[13] J. Chakaya, E. Petersen, R. Nantanda, B.N. Mungai, G.B. Migliori, F. Amanullah, A. Zumla, The WHO global tuberculosis 2021 report–not so good news and turning the tide back to end TB, Int. J. Infect. Dis. 124 (2022) S26–S29.
[14] M.M. Dehmer, N.N. Barbarini, K.K. Varmuza, A.A. Graber, Novel topological descriptors for analyzing biological networks, BMC Struct. Biol. 10 (1) (2010) 1–17.
[15] E. Estrada, L. Torres, L. Rodriguez, I. Gutman, An atom-bond connectivity index: modelling the enthalpy of formation of alkanes, Indian J. Chem. 37A (1998) 849–855.
[16] I. Euldji, A. Belghait, C. Si-Moussa, O. Benkortbi, A. Amrane, A new hybrid quantitative structure property relationships-support vector regression (QSPR-SVR) approach for predicting the solubility of drug compounds in supercritical carbon dioxide, AIChE J. (2023) e18115.
[17] C. Fernandez-Lozano, M. Gestal, N. Pedreira-Souto, L. Postelnicu, J. Dorado, C. Robert Munteanu, Kernel-based feature selection techniques for transport proteins based on star graph topological indices, Curr. Top. Med. Chem. 13 (14) (2013) 1681–1691.
[18] P.J.I. Feng, D.J. Horne, J.M. Wortham, D.J. Katz, CDC tuberculosis epidemiologic studies consortium. Trends in tuberculosis clinicians' adoption of short-course regimens for latent tuberculosis infection, J. Clin. Tuberc. Other Mycobact. Dis. (2023) 100382.
[19] J.L. Flynn, J. Chan, Immune cell interactions in tuberculosis, Cell 185 (25) (2022) 4682–4702.
[20] I. Gutman, N. Trinajstić, Graph theory and molecular orbitals: total π-electron energy of alternant hydrocarbons, Chem. Phys. Lett. 17 (1972) 535–538.
[21] I. Gutman, Degree-based topological indices, Croat. Chem. Acta 86 (4) (2013) 351–361.
[22] M. Kaforou, C. Broderick, O. Vito, M. Levin, T.J. Scriba, J.A. Seddon, Transcriptomics for child and adolescent tuberculosis, Immunol. Rev. 309 (1) (2022) 97–122.
[23] S. Kavitha, S. Varuna, R. Ramya, A comparative analysis on linear regression and support vector regression, in: 2016 Online International Conference on Green Engineering and Technologies (IC-GET), IEEE, 2016, pp. 1–5.
[24] A. Khan, S. Hayat, Y. Zhong, A. Arif, L. Zada, M. Fang, Computational and topological properties of neural networks by means of graph-theoretic parameters, Alex. Eng. J. 66 (2023) 957–977.
[25] A. Konstantinos, Testing for tuberculosis, Aust. Prescr. 33 (2010) 12–18, https://doi.org/10.18773/austprescr.2010.005.
[26] I. Masmali, M. Naeem, M. Ishaq, A.N.A. Koam, Estimation of the physiochemical characteristics of an antibiotic drug using M-polynomial indices, Ain Shams Eng. J. 14 (11) (2023) 102539.
[27] K.A. Molla, M.A. Reta, Y.Y. Ayene, Prevalence of multidrug-resistant tuberculosis in East Africa: a systematic review and meta-analysis, PLoS ONE 17 (6) (2022) e0270272.
[28] S. Mondal, A. Dey, N. De, A. Pal, QSPR analysis of some novel neighbourhood degree-based topological descriptors, Complex Intell. Syst. 7 (2) (2021) 977–996.
[29] S. Mondal, N. De, A. Pal, On some new neighbourhood degree based indices, Acta Chem. Iasi 27 (1) (2019) 31–46.
[30] C.R. Munteanu, H. González-Díaz, F. Borges, A.L. de Magalhães, Natural/random protein classification models based on star network topological indices, J. Theor. Biol. 254 (4) (2008) 775–783.
[31] S. Nikolic, G. Kovacevic, A. Milicevic, N. Trinajstic, Degree-based topological indices, Croat. Chem. Acta 76 (2) (2003) 113–124.
[32] F.J. Osaye, A. Alochukwu, Covid-19 pandemic model: a graph theoretical perspective, in: Advances in Epidemiological Modeling and Control of Viruses Academic Press, 2023, pp. 285–303.
[33] R. Todeschini, V. Consonni, Molecular Descriptors for Chemoinformatics: Volume I: Alphabetical Listing / Volume II: Appendices, References, Volume III: Appendices, References, Wiley-VCH, 2009.
[34] S. Parveen, N.U. Hassan Awan, M. Mohammed, F.B. Farooq, N. Iqbal, Topological indices of novel drugs used in diabetes treatment and their QSPR modeling, J. Math. (2022) 1–17.
[35] M. Randić, On characterization of molecular branching, J. Am. Chem. Soc. 157 (97) (1975) 6609–6615.
[36] M.C. Shanmukha, N.S. Basavarajappa, K.C. Shilpa, A. Usha, Degree-based topological indices on anticancer drugs with QSPR analysis, Heliyon 6 (2020) e04235.
[37] A.M. Ulugbek o'gli, Factors predicting mortality in pulmonary tuberculosis, Cent. Asian J. Med. Nat. Sci. 3 (3) (2022) 362–367.
[38] M. Van Schalkwyk, A. Bekker, E. Decloedt, J. Wang, G.B. Theron, M.F. Cotton, et al., Pharmacokinetics and safety of first-line tuberculosis drugs rifampin, isoniazid, ethambutol, and pyrazinamide during pregnancy and postpartum: results from IMPAACT P1026s, Antimicrob. Agents Chemother. 67 (11) (2023) e0073723.
[39] D. Vukičević, B. Furtula, Topological index based on the ratios of geometrical and arithmetical means of end-vertex degrees of edges, J. Math. Chem. 46 (4) (2009) 1369–1376.
[40] H. Wiener, Structural determination of paraffin boiling points, J. Am. Chem. Soc. 1 (69) (1947) 17–20.
[41] S. Yang, W. Lu, N. Chen, Q. Hu, Support vector regression based QSPR for the prediction of some physicochemical properties of alkyl benzenes, J. Mol. Struct., Theochem 719 (1–3) (2015) 119–127.
[42] S.S. Yang, W.C. Lu, T.H. Gu, L.M. Yan, G.Z. Li, QSPR study of n-octanol/water partition coefficient of some aromatic compounds using support vector regression, QSAR Comb. Sci. 28 (2) (2009) 175–182.
[43] M.A. Zaid, Correlation and Regression Analysis Textbook, The Statistical, Economical and Social Research and Training Centre for Islamic Countries (SESRIC), Oran, Ankara, 2015.
[44] S. Zaman, W. Ahmed, A. Sakeena, Mathematical modeling and topological graph description of dominating David derived networks based on edge partitions, Sci. Rep. 13 (2023) 15159, https://doi.org/10.1038/s41598-023-42340-6.
[45] Y.P. Zhou, J.H. Jiang, W.Q. Lin, H.Y. Zou, H.L. Wu, G.L. Shen, R.Q. Yu, Boosting support vector regression in QSAR studies of bioactivities of chemical compounds, Eur. J. Pharm. Sci. 28 (2006) 344–353.
[46] J.F. Zhong, A. Rauf, M. Naeem, J. Rahman, A. Aslam, Quantitative structure-property relationships (QSPR) of valency based topological indices with Covid-19 drugs and application, Arab. J. Chem. 14 (2021) 103240.
[47] Short Report, The First National TB Prevalence Survey, South Africa, 2018.
[48] Global Tuberculosis Report, World Health Organization, 2022.
[49] World Health Organization, Use of high burden country lists for TB by WHO in the post, Geneva, 2015.